Miró-Mur F, Pérez-de-Puig I, Ferrer-Ferrer M, Urra X, Justicia C, Chamorro A, Planas AM.

Immature monocytes recruited to the ischemic mouse brain differentiate into macrophages with features of alternative activation.

Brain Behav Immun. 2015 Aug 12.

pii: S0889-1591(15)00434-1. doi: 10.1016/j.bbi.2015.08.010.

Immature monocytes recruited to the ischemic mouse brain differentiate into macrophages with features of alternative activation

Francesc Miró-Mur[1,&], Isabel Pérez-de Puig[1,2,&], Maura Ferrer-Ferrer[1,2], Xabier Urra[1,3], Carles Justicia[1,2], Angel Chamorro[1,3], and Anna M. Planas[1,2*]

[1] Àrea de Neurociències, Institut d'Investigacions Biomèdiques August Pi i Sunyer (IDIBAPS), 08036-Barcelona, Spain

[2] Departament d'Isquèmia Cerebral i Neurodegeneració, Institut d'Investigacions Biomèdiques de Barcelona (IIBB), Consejo Superior de Investigaciones Científicas (CSIC), 08036-Barcelona, Spain

[3] Functional Stroke Unit of Cerebrovascular Diseases, Hospital Clínic, 08036-Barcelona, Spain

[&] These authors equally contributed to this work.

* Corresponding author:

Anna M. Planas
IIBB-CSIC, IDIBAPS
Rosselló 161, planta 6
08036-Barcelona, Spain
e-mail: anna.planas@iibb.csic.es
Tel: +34-93 363 83 27
Fax: +34-93 363 83 01

Abbreviated title: Fate of monocytes in the ischemic brain tissue

Abstract

Acute stroke induces a local inflammatory reaction causing leukocyte infiltration. Circulating monocytes are recruited to the ischemic brain and become tissue macrophages morphologically indistinguishable from reactive microglia. However, monocytes are a heterogeneous population of cells with different functions. Herein, we investigated the infiltration and fate of the monocyte subsets in a mouse model of focal brain ischemia by permanent occlusion of the distal portion of the middle cerebral artery. We separated two main subtypes of $CD11b^{hi}$ monocytes according to their expression of the surface markers Ly6C and CD43. Using adoptive transfer of reporter monocytes and monocyte depletion, we identified the pro-inflammatory $Ly6C^{hi}CD43^{lo}CCR2^{+}$ subset as the predominant monocytes recruited to the ischemic tissue. Monocytes were seen in the leptomeninges from where they entered the cortex along the penetrating arterioles. Four days post-ischemia, they had invaded the infarcted core, where they were often located adjacent to blood vessels. At this time, Iba-1^{-} and Iba-1^{+} cells in the ischemic tissue incorporated BrdU, but BrdU incorporation was rare in the reporter monocytes. The monocyte phenotype progressively changed by down-regulating Ly6C, up-regulating F4/80, expressing low or intermediate levels of Iba-1, and developing macrophage morphology. Moreover, monocytes progressively acquired the expression of typical markers of alternatively activated macrophages, like arginase-1 and YM-1. Collectively, the results show that stroke mobilized immature pro-inflammatory $Ly6C^{hi}CD43^{lo}$ monocytes that acutely infiltrated the ischemic tissue reaching the core of the lesion. Monocytes differentiated to macrophages with features of alternative

activation suggesting possible roles in tissue repair during the sub-acute phase of stroke.

1. INTRODUCTION

Brain ischemia induces neuronal cell death and inflammation that attracts circulating leukocytes to the injury site (Gelderblom et al., 2009, Chu et al., 2014). Several lines of evidence support that monocytes can promote further inflammation and exacerbate the brain lesion in acute stroke (Dimitrijevic et al., 2007). However, they seem to exert beneficial effects in the sub-acute phase of stroke by preventing hemorrhagic transformation (Gliem et al., 2012). Identification of monocytes infiltrated in the ischemic tissue is tricky since they become morphologically indistinguishable from the population of reactive resident microglia. Furthermore, circulating monocytes are a heterogeneous population of cells composed of various subsets with different phenotypes (Strauss-Ayali et al., 2007). In humans, the majority of monocytes are $CD14^+$ $CD16^-$, but there is a minority of monocytes expressing different levels of CD16 that change their proportions in response to acute stroke (Urra et al., 2009). Mouse monocytes express cell surface molecules that are different from those of human monocytes, but functional equivalences between mouse and human monocytes have been proposed making use of the mouse surface marker lymphocyte antigen 6 complex, locus C (Ly6C), and leukosialin, also known as sialophorin or cluster of differentiation 43 (CD43) (Geissmann et al., 2003; Strauss-Ayali et al., 2007; Sunderkötter et al., 2004; Ziegler-Heitbrock et al., 2010). Ly6C is anchored to the cell surface via a phosphatidylinositol moiety and upon cross-linking initiates cell stimulation (Bamezai et al., 1989). CD43 is a sialylated glycoprotein binding to CD54 (ICAM-1) and E-selectin (Merzaban et al., 2011; Zarbock et al., 2011), and playing complex roles in cell-cell and cell-endothelium interactions by

exerting either pro-adhesive or anti-adhesive actions (Ostberg et al., 1998) and facilitating cell infiltration (Woodman et al., 1998). Mouse monocytes with high expression of CD43 are classified as 'non-classic' or 'intermediate' monocytes with functional equivalence to $CD16^+$ human monocytes (Ziegler-Heitbrock et al., 2010). Comparatively, the $Ly6C^{hi}CD43^{lo}$ monocytes are considered pro-inflammatory due to their high production of TNF-α and IL-1β (Ziegler-Heitbrock et al., 2010). In stroke patients, an increased proportion of classic $CD14^{hi}CD16^-$ circulating monocytes on admission was associated with early clinical worsening, poor outcome and mortality at day 90 (Urra et al., 2009), suggesting that the classic monocytes could play some deleterious role. However, the specific monocyte subtypes that infiltrate the ischemic brain, as well as their function and fate, are not well characterized after ischemia in the absence of reperfusion. Here we studied the features of circulating monocyte subsets after permanent brain ischemia, their infiltration to the ischemic brain tissue, and their fate.

2. MATERIALS AND METHODS

2.1 Animals

Animal work was performed according to our local regulations in compliance with the Spanish legislation (Real Decreto 53/2013) and European Community Directives, and following the ARRIVE guidelines. The Ethical Committee (CEEA) of the University of Barcelona approved the experimental

procedures. Brain ischemia was induced in adult (3-4 months) male C57BL/6j mice (Charles River, Lyon, France). C57BL/6j mice carrying the CD45.1 allele (Ly5.1) (B6.SJL-Ptprc Pepc/BoyJ) and transgenic C57BL/6 mice expressing the red fluorescent protein DsRed under the control of the β-actin promoter were used to obtain reporter monocytes for adoptive transfer experiments.

2.2 Brain ischemia

Permanent distal occlusion of the right middle cerebral artery (MCAo) was carried out under isoflurane anaesthesia in 30% O_2 and 70% N_2O, as reported (Pérez-de-Puig et al., 2013). In brief, after drilling a small hole in the cranium at the level of the distal portion of the MCA, the artery was occluded by cauterization. Flow obstruction was visually verified. After surgery, animals were allowed to recover from the anaesthesia and were returned to their cages. None of the animals died after MCAo. In a group of mice, MRI ($T2_w$) was carried out in a 7.0T horizontal animal scanner (BioSpec, Bruker BioSpin, Ettlingen, Germany), equipped with a 12 cm inner diameter actively shielded gradient system (400 mT/m), as described (Pérez-de-Puig et al., 2013).

2.3 Isolation of blood leukocytes

In anesthetized animals, blood was extracted from the cava vein and collected in EDTA tubes (1.6 mg EDTA/mL blood; Micro tube 1.3 mL K3E, Sarstedt) for analysis. Five-hundred µL of total blood were incubated for 10 min with 5 mL of red blood cell (RBC) lysis solution (150 mM NH_4Cl, 10 mM $KHCO_3$, 0.1 mM EDTA). Cells were centrifuged at 800 *x g* for 5 min and washed in 10 mL of cold PBS. Leukocytes were finally collected in fluorescence-activated cell

sorting (FACS) buffer (PBS, 2 mM EDTA, 2% FBS) for flow cytometry analysis.

2.4 Isolation of brain cells

Mice were anesthetized and perfused transcardially with 40 mL saline containing heparin (5U/mL). The ischemic cortex (ipsilateral) and the corresponding region of the non-affected hemisphere (contralateral) were dissected out and analysed separately. The tissue was incubated for 20 min at 37°C in 2 mL of RPMI 1640 (Life Technologies S.A., Alcobendas, Madrid, Spain) containing 100 U/mL collagenase IV and 50 U/mL DNAse I. Brain tissue was passed through a tissue grinder and cells were recovered after centrifugation at 400 x *g* for 10 min and separated from myelin and debris in 70 % and 30 % isotonic percoll gradient (GE Healthcare) in Hank's Balanced Salt Solution (HBSS) without calcium or magnesium. Samples were centrifuged at 1,000 x *g* for 30 min without acceleration or brake. Cells were collected from the interface, washed once with HBSS, and processed for flow cytometry.

2.5 Isolation of monocytes from the bone marrow

Monocytes were extracted from the CD45.1 mice or the transgenic DsRed mice. Mice were killed by isofluorane overdose, the femurs and tibiae from hindlimbs were removed, cleaned of all connective tissue and placed on 5 mL cold PBS. In sterilized conditions, bones were washed with 70% ethanol and placed in complete media, i.e. RPMI 1640 medium (Life Technologies S.A.), containing 10% FBS. The ends of each tibia and femur were clipped to

expose the bone marrow, and bone marrow cells were flushed from bones into medium using a syringe with a 23-gauge needle. The cell suspension was passed through a 70 μm nylon mesh strainer and centrifuged at 300 *x g* for 6 min. Monocytes were enriched by using the EasySep negative selection mouse monocyte enrichment kit (StemCell Technologies, Grenoble, France). Briefly, cells were resuspended at 1 x 10^8 cells/mL in FACS buffer with 5% rat serum and incubated for 15 min at 4°C with EasySep® Mouse Enrichment Cocktail at 50 μL/mL. A wash was carried out with FACS Buffer and centrifuged at 300 *x g* for 10 min. Cells were resuspended at 1 x 10^8 cells/mL in FACS buffer and incubated with EasySep®Biotin Cocktail at 60 μL/mL for 15 min at 4°C. Cells were incubated for 10 min with EasySep® Magnetic Particles at 150 μL/mL. FACS buffer was added to a final volume of 2.5 mL and the sample tube was placed in the EasySep® magnet for 5 min. The desired fraction was poured off into a new tube and centrifuged 300 *x g* for 10 min. Isolated monocytes expressed high levels of Ly6C ($Ly6C^{hi}$) and their purity was above 90%.

2.6 Flow cytometry

Isolated brain and blood cells were washed with FACS buffer, incubated at 4°C for 10 min with FcBlock (1/200; Clone 2.4G2; BD Pharmingen), and incubated with primary antibodies in FACS buffer for 30 min at 4°C. The antibodies used were rat anti-mouse CD11b (clone M1/70, Alexa Fluor 647, BD Pharmingen), CD45 (clone 30-F11, FITC, BD Pharmingen), Ly6G (clone 1A8, PE-Cy7, BD Pharmingen), CD45.1 (clone A20, V450, BD Horizon; or APC, Tonbo Biosciences), Ly6C (clone ER-MP20, FITC, Abcam; or clone

HK1.4, eFluor450, eBioscience), CD43 (clone S7, PE, BD Pharmingen), CD11c (clone HL3, PE, BD Pharmingen), MHCII (clone M5/114.15.2, PerCP, Biolegend), and CCR2 (475301, fluorescein, R&D). For intracellular staining (ICS) in flow cytometry, after surface staining, cells were incubated in fixation buffer (Biolegend) at room temperature for 20 min, and permeabilized with permeabilization wash buffer (Biolegend) at room temperature for 20 min. Additional incubation with an antibody against arginase-1 (Arg-1) (sheep polyclonal, PE, R&D Systems) diluted in the permeabilization wash buffer was carried out for 30 min. Isotype controls were rat IgG2bκ (clone A95-1, Alexa Fluor 647 or FITC, BD Pharmingen), rat IgG2a (FITC, Hycult Biotech), and rat IgG2aκ (clone R35-95, PE-Cy7, BD Pharmingen). Data was acquired in a BD FacsCanto II cytometer using the FacsDiva software (BD Biosciences). Cells were morphologically identified by linear forward scatter (FSC-A) and side scatter (SSC-A) parameters, as described (Pérez-de-Puig et al., 2013). Data analysis was performed with FlowJo software (version 7.6.5, TreeStar Inc., Ashland, OR, USA). Again, cells were plotted on forward versus side scatter and single cells were gated on FSC-A versus FSC-H linearity. Flow-Count Fluorospheres (Beckman-Coulter) were used for absolute quantification.

2.7 Separation of monocyte subtypes by cell sorting

Blood was collected from the cava vein in EDTA tubes. Spleens were dissected in 1 mL RPMI-1604 medium and pressed through a 40 μm-cell strainer (BD Bioscience). Cells were incubated for 5 min in RBC lysis buffer and washed twice in PBS. Blood was treated as indicated above. Leukocytes from spleen and blood were stained for flow cytometry with CD11b-Alexa

Fluor 647, Ly6G-PE/Cy7 and Ly6C-FITC. Monocytes were sorted in a FACSAria cytometer (BD Biosciences) by gating on $CD11b^{hi}Ly6G^{-}$ cells. Cells were collected in complete RPMI-1640 medium and purity was above 95 % for both subtypes.

2.8 Adoptive transfer experiments

Monocytes isolated from the bone marrow of reporter donor mice expressing the CD45.1 marker or transgenic DsRed mice were adoptively transferred to recipient C57BL/6j mice. 1.5 x 10^6 monocytes in 250 µl PBS were injected through the caudal vein at different time points after MCAo. Reporter monocytes were transferred to the recipient mice either at 3 hours, 1, 3, or 6 days post-ischemia, as stated in each particular experiment.

2.9 Depletion of circulating monocytes

Clodronate liposomes (ClodronateLiposomes.com, Haarlem, The Netherlands) were injected i.v. according to the manufacturer specifications. Injection was carried out in control mice (n=6) and 1 day prior to MCAo (n=10). For treatment controls, mice received phosphate-buffered saline (PBS) liposomes as the vehicle 1 day before MCAo (n=6).

2.10 Immunofluorescence

Mice were perfused through the heart with saline followed by 4% paraformaldehyde (PFA) in phosphate buffer (PB) pH 7.4. The brain was removed, fixed overnight with the same fixative, and immersed in 30 % sucrose in PB for cryoprotection and frozen in isopentane at -40 ºC. Cryostat brain sections (14-µm-thick) were fixed in ethanol, blocked with normal serum,

and incubated overnight at 4º C with primary antibodies: goat polyclonal antibodies against Arg-1 (1:100, #sc-18354, Santa Cruz Biotechnology Inc., Santa Cruz, CA, USA) or α-4-laminin (1:20, #AF3837, R&D Systems, Inc., Minneapolis, MN, USA), rabbit polyclonal antibody against YM-1 (1:100, #1404, Stemcell Technologies, Vancouver, Canada), ionized calcium-binding adapter molecule-1 (Iba-1) (1:100, #016-20001, Wako Chemicals GmbH, Neuss, Germany) or pan-laminin (1:100, #Z0097, DAKO, Dako Diagnósticos, S.A., Sant Just Desvern, Spain), mouse monoclonal antibody anti-CD45.1 (1:200, clone A20, BD Pharmingen), and rat monoclonal antibody against CD68 (1:100; #MCA1957, Abd Serotec, Bio-Rad), followed by secondary antibodies (Alexa Fluor® 488, 546, or 647; Molecular Probes; Life Technologies S.A). To identify astrocytes we used a mouse monoclonal antibody against GFAP conjugated with Alexa Fluor-546 (#8152; Cell Signalling Technology, Danvers, MA, USA) diluted 1:50. The brain DsRed signal was detected in the window between 556-600 nm. To amplify the signal of the DsRed cells, in certain experiments we used a rabbit polyclonal anti-red fluorescent protein (RFP) antibody (#ab34771; Abcam) diluted 1:100 or a goat polyclonal anti-DsRed antibody (#sc-33354, Santa Cruz Biotechnology, Inc.) diluted 1:100, followed by a secondary antibody (Alexa Fluor® 546). We used brain sections from ischemic mice not injected with DsRed cells as negative controls. Cell nuclei were stained with Hoechst or To-Pro3 (Invitrogen) (shown in blue). Images were obtained by confocal microscopy (SP5 or TCS SPE-II, Leica Microsystems) with the LAS software (Leica) and were not further processed excepting for enhancing global signal intensity in the entire images using the LAS or Adobe photoshop software for image presentation purposes.

Cell counting was carried out after obtaining at least three pictures of the immunostainings (objective x40) in three different brain sections per mouse. Unless otherwise stated, values are expressed as the mean±SD of n mice per experiment, as described in the figure legends.

2.11 In vivo BrdU incorporation

Bromodeoxyuridine (BrdU) (10 mg/mL) in sterile PBS (#550891, BD Pharmingen) was injected i.p. (150 µl) into ischemic mice as a single dose at day 2 or 4 after MCAo and one hour later mice were killed. The brain was processed as for immunofluorescence or flow cytometry (see above). Cryostat brain sections were fixed in 1% PFA, washed in PBS and then 3 times in borate buffer (pH 8.5) followed by 3 washes in PBS. Sections were denatured in 2M HCl for 30 min at 37ºC and then incubated with a rat monoclonal FITC-anti-BrdU antibody (BU1/75 (ICR1), #ab74545, Abcam) diluted 1:50.

2.12 qRT–PCR

Total RNA was extracted (Purelink RNA Kit, Invitrogen) and RNA quantity and purity was determined (ND-1000 micro-spectrophotometer, NanoDrop Technologies, Wilmington, DE, USA). One-µg of total RNA was reverse transcribed using a mixture of random primers (High Capacity cDNA Reverse Transcription kit, Applied Biosystems, Life Technologies S.A.). Housekeeping gene for normalization was succinate dehydrogenase complex subunit A (SDHA). We used the following PCR primers (IDT, Laboratorios Conda S.A., Torrejon de Ardoz, Spain) that were designed (Primer3 software) to bridge the exon–intron boundaries within the gene of interest: Arg-1 (ANM_007482.3) F:

AGGGTTACGGCCGGTGGAGAG, R: CCTCAGTGCTGCAGGGCCTTT; YM-1 (NM_009892.2) F: CAGGTCTGGCAATTCTTCTGAA, R: GTCTTGCTCATGTGTGTAAGTGA; CCL-2 (NM_011333.3) F: AGGTGTCCCAAAGAAGCTGTAG, R: AATGTATGTCTGGACCCATTCC; and SDHA (NM_023281.1) F: TGGGGAGTGCCGTGGTGTCA, R: CATGGCTGTGCCGTCCCCTG. Real-time quantitative RT–PCR analysis was performed by SYBR green I dye detection (#11761500; Invitrogen) using the iCycler iQTM Multicolor Real-Time Detection System (Bio-Rad, Hercules, CA, USA). Optimized thermal cycling conditions were as previously reported (Pérez-dePuig et al., 2013). Data were collected after each cycle and were graphically displayed (iCycler iQTM Real-time Detection System Software, version 3.1; Bio-Rad). Melt curves were carried out on completion of the cycles to ensure product amplification specificity. Quantification was performed using the standard dilution calibration curve and values were normalized to the reference gene. Values are expressed as fold versus mean (n=3 to 6) control brain samples.

2.13 ELISA immunoassays

For immunoassays in brain tissue, mice were anesthetized and perfused through the heart with ice-cold Hanks balanced salt solution (Invitrogen, Life Technologies S.A.). The ipsilateral and contralateral cortices were dissected out and processed as reported (Cardona et al., 2008). Sorted mouse monocytes expressing $Ly6C^{hi}$ or $Ly6C^{lo}$ were cultured in 96-well round bottom plate at 12.5 x 10^4 cells/mL for 18 h at 37º C in 5% CO_2 with or without 100 ng/mL LPS. The concentration of cytokines and chemokines was measured

using the Bio-plex ELISA assays (Bio-Plex Pro-Mouse Cytokine 23-Plex, group I; Bio-Rad). Data acquisition was carried out in a Luminex system (Life Technologies) with luminex xPONENT software, and data analysis was performed using Bio-Plex Manager software (Bio-Rad).

2.14 Statistical Analyses

Two-group comparisons were carried out with the Mann-Whitney *U* test or the *t*-test, as required after testing for normality. Multiple groups were compared with one-way ANOVA or two-way ANOVA followed by the Bonferroni test, or the Dunnett's test for comparison against controls. Unless otherwise stated, values in graphs are expressed as the mean±SEM. Statistical analyses were performed using GraphPad software (GraphPad Software Inc., La Jolla, CA).

3. RESULTS

3.1 The majority of monocytes infiltrated to the ischemic brain tissue are Ly6C^{hi}CD43^{lo}

Classic CD11b^{hi}Ly6C^{hi} monocytes in the mouse blood show low expression of CD43 (CD43^{lo}) and are CCR2^{+}, whereas CD11b^{hi}Ly6C^{lo}CD43^{hi} monocytes are CCR2^{-} and express MHCII and CD11c (Fig. 1A, see Supplementary Fig. 1 for gating strategy). *Ex vivo* studies of monocyte subsets isolated from the blood using positive cell sorting with Ly6C (Supplementary Fig. 2) showed that non-classic Ly6C^{lo} monocytes produced less cytokines and released less

chemokines than the classic Ly6C^{hi} monocytes, both under basal conditions and after stimulation (Supplementary Fig. 3).

The Ly6C^{hi}CD43^{lo} monocytes are CCR2^{+} and therefore are expected to respond to the chemokine CCL2, which was induced in the ischemic brain (Fig. 1B, C), in agreement with previous reports (e.g. Wang et al., 1995). In order to identify the monocyte subsets that infiltrate into the ischemic brain tissue, myeloid cells were studied in the brain up to 7 days after middle cerebral artery occlusion (MCAo) (for gating strategy see Supplementary Fig. 4). A prominent population of CD11b^{hi}CD45^{hi} cells was found in the ipsilateral but not the contralateral brain hemisphere (Fig. 1D). After excluding the Ly6G^{+} neutrophils, most of the remaining CD11b^{hi}CD45^{hi} myeloid cells were further characterized as Ly6C^{hi}CD43^{lo} monocytes, while only low numbers of Ly6C^{lo}CD43^{hi} monocytes were detected (Fig. 1E). Therefore, the population of monocytes that predominantly infiltrated the ischemic tissue was the classic Ly6C^{hi}CD43^{lo} subtype.

We depleted circulating monocytes with clodronate liposomes (Bauer et al., 1995) to verify that the cells identified in the brain as CD11b^{hi}CD45^{hi}Ly6C^{hi}CD43^{lo} were actually derived from the circulation. Treatment strongly reduced the population of blood CD11b^{hi} monocytes, both Ly6C^{hi} and Ly6C^{lo}, one day after administration but at day 2 the numbers of circulating Ly6C^{hi} cells recovered, while the Ly6C^{lo} population remained lower than control (Supplementary Fig. 5). Thus, i.v. injection of clodronate liposomes acutely depleted circulating monocytes, but in turn it stimulated the

progressive release of Ly6C^{hi} monocytes to the circulation from body reservoirs. Intravenous administration of clodronate liposomes does not affect brain microglia under control conditions (Bauer et al., 1995; Polfliet et al., 2001). However, the fact that the blood-brain barrier (BBB) is damaged after stroke (Yang and Rosenberg, 2011), let us to deduce that passive leakage of clodronate liposomes from the blood to the brain could take place if the drug was administered after stroke. To avoid any direct effects on microglia, we administered the drug i.v. one day before MCAo. The population of resident microglia cells, defined as CD11b^{dim}CD45^{lo} (Campanella et al, 2002; Cardona et al., 2006), was not affected (Fig. 1F). In contrast, clodronate liposomes reduced the numbers of infiltrated myeloid cells (Fig. 1G), particularly affecting the CD11b^{hi}CD45^{hi}Ly6C^{hi} cells (Fig. 1H), demonstrating that they were blood-born monocytes.

3.2 Blood-born monocytes change their phenotype in the brain tissue

In order to follow up the monocytes infiltrated into the ischemic tissue, we carried out adoptive transfer of reporter CD45.1^{+} monocytes obtained from the bone marrow of Ly5.1 congenic donor mice into regular wild type (Ly5.2) mice expressing the CD45.2 allele. The reporter CD45.1^{+} monocytes sorted from the bone marrow were mainly Ly6C^{hi} (>90%) (Supplementary Fig. 6). These reporter monocytes were transferred to the recipient mice after MCAo (Fig. 2A) and were differentiated from the endogenous wild type CD45.2 monocytes by flow cytometry using an anti-CD45.1 antibody (Fig. 2B and Supplementary Fig. 7). The day after injection, circulating CD45.1^{+} monocytes kept their original Ly6C^{hi}CD43^{lo} phenotype, but four days later, all the CD45.1^{+}

cells became Ly6C^{lo}CD43^{hi} (Supplementary Fig. 8), showing the maturation of bone-marrow-derived immature monocytes in the blood.

Given that infiltrated cells peaked in the brain at day four post-ischemia (Fig. 1D), CD45.1 monocytes were initially administered at day 3 post-ischemia and the brain tissue was studied by flow cytometry 1 and 4 days later (Fig. 2C). CD45.1^{+} cells were found in the ischemic tissue (Fig. 2D) but not in the contralateral hemisphere or in the control non-ischemic brain tissue (not shown). The infiltrated CD45.1^{+} cells were Ly6C^{hi}CD43^{lo}, while Ly6C^{lo}CD43^{hi} CD45.1^{+} cells were hardly detected (Fig. 2E). By immunofluorescence and confocal microscopy, we detected isolated CD68^{+}CD45.1^{+} cells in the ischemic territory, but not in the contralateral non-ischemic hemisphere (Fig. 2F). In a separate experiment, we checked that monocyte administration did not significantly affect the natural progression of the initial brain lesion, as assessed with longitudinal MRI ($T2_w$) (Fig. 2G).

Altogether, these findings further demonstrated that circulating classic Ly6C^{hi}CD43^{lo} monocytes were the predominant monocyte subtype recruited to the ischemic brain tissue. However, the percentage of CD45.1^{+} cells showing Ly6C^{hi} expression in the tissue decreased from 1 to 4 days following administration (Fig. 2H), suggesting that the infiltrated Ly6C^{hi} monocytes progressively down-regulated the surface expression of Ly6C in the tissue but they did not up-regulate CD43, in contrast to their maturation in the blood where down-regulation of Ly6C is accompanied by up-regulation of CD43 (Supplementary Fig. 8).

3.3 Fate of infiltrated Ly6C^{hi} monocytes

The above results suggested that the environment of the damaged brain tissue favored the loss of typical blood monocyte features. To investigate whether the infiltrated monocytes acquired characteristics of tissue macrophages, we examined the expression of the typical macrophage marker F4/80. The numbers of CD11b^{+}F4/80^{+} cells increased in the brain tissue after MCAo (Fig. 3A). Systemic administration of clodronate liposomes one day prior to MCAo reduced the numbers of CD11b^{+}F4/80^{+} cells in the ischemic tissue at day 4 (Fig. 3A). Furthermore, the percentage of CD11b^{hi}CD45^{hi}Ly6G^{-} cells expressing F4/80 was higher in the brain than in the blood, and so was the mean fluorescence intensity (MFI) (Fig. 3B). Furthermore, after adoptive transfer of reporter Ly6C^{hi}CD45.1 monocytes, again the percentage of CD45.1 monocytes expressing F4/80 (Fig. 3C) and the MFI of F4/80^{+} CD45.1 monocytes (Fig. 3C) was higher in brain than blood. We concluded that infiltrated monocytes progressively up-regulated F4/80 in the ischemic tissue showing that they differentiated to macrophages.

To further investigate the fate of the infiltrated monocytes, we obtained reporter Ly6C^{hi} monocytes form the bone marrow of DsRed transgenic mice. The red fluorescent reporter monocytes were injected into recipient wild type mice three days after MCAo, as before. Given that monocytes can reach the brain tissue during the first hours post-ischemia (Chu et al., 2014), another group of mice received monocyte transfer one day after ischemia. The blood and the brain were studied at day 2 or 4 after MCAo. DsRed^{+} cells were found in the blood and the ischemic tissue by flow cytometry (Supplementary Fig. 9). Confocal microscopy allowed the identification of the DsRed cells in the

ischemic tissue (Fig. 3D) while they were not seen in the contralateral hemisphere (not shown). By counting the number of DsRed cells in relation to the cell nuclei in the ischemic core four days after MCAo following DsRed cell injection at day 1 post-ischemia, we estimated that the DsRed cells in the ischemic core corresponded to less than 1%. The morphology of some of the DsRed cells found in the brain was compatible with monocytes, while others showed a macrophage-like morphology (Fig. 3D), and the proportion of the latter increased from day 1 to 3 following administration of the reporter monocytes.

3.4 The reporter monocytes associate to blood vessels

DsRed monocytes injected the day after MCAo were found one day later in the area of the leptomeninges, on the basement membrane of the cortex and in the superficial cortical layers along the paths of the arterioles penetrating the infarcted cortex (Fig. 4 A-D). DsRed cells were often seen adjacent to the parenchymal side of the endothelial basal lamina of the blood vessels (Fig. 4 E-L). In some cases the cells were very flat and extended along the basal lamina suggesting a perivascular location (Fig. 4H-I). DsRed cells were also found separated from the vessels (Fig. 4J-K) and were seen in the track of capillaries that appeared broken due to discontinuation of the endothelial basal lamina (α4-laminin) (Fig. 4L), possibly due to protease degrading activity around the blood vessels within the infarcted core. Using antibodies against pan-laminin, DsRed cells were detected in the internal (Fig. 4M) and external (Fig. 4 N-Q) sides of the parenchymal basal lamina. By counting the numbers of DsRed monocytes associated to the vessels or in the parenchyma

at different time points after cell administration, it became apparent that the cells progressively detached from the vascular network (Fig. 4R).

3.5 Infiltrated monocytes become Iba-1$^+$

Brain resident microglia cells express Iba-1 and up-regulate the expression of this protein when they become reactive. By immunofluorescence, the highest level of intensity of Iba-1 expression 4 and 7 days post-ischemia was found in cells at the edge of the ischemic core whereas cells within the core expressed comparatively lower levels of Iba-1, and the density of Iba-1$^+$ cells was significantly higher at the border of the infarction than in the core ($p<0.05$) (Fig. 5A-C). Following injection of the DsRed monocytes, DsRed cells were seen in the leptomeninges and superficial cortical zones, and they reached deeper cortical layers at the margins of the infarction at 2 and 4 days post-ischemia (Fig. 5A), progressively reaching the core of the infarction (Fig. 5C). We estimated that the proportion of DsRed cells that were Iba-1$^+$ increased from 40% to 70% at one (Fig. 5C) and three (Fig. 5D-H) days after administration, respectively, suggesting that the monocytes up-regulated the expression of Iba-1 after brain infiltration. Morphologically, these Iba-1$^+$ DsRed monocytes could not be distinguished from other neighboring Iba-1$^+$ endogenous cells (Fig. 5).

3.6 Infiltrated monocytes are not highly proliferative

The population of macrophage-like cells in the ischemic tissue increases during the first days post-ischemia. We asked whether cell proliferation was

involved in the expansion of the monocyte population by injecting BrdU after ischemia showing the cells that were in the S-phase of the cell cycle at that time. Two days after MCAo, the core of the lesion was completely surrounded by $BrdU^+$ cells (Fig. 6A) that were not seen in the contralateral hemisphere, excepting the periventricular zone (not shown). $BrdU^+$ cells were found in extensive cortical zones at the edges of the ischemic core (Fig. 6A) and they were prominent on the cortical basement membrane and following the paths of the penetrating arterioles (Fig. 6B). However, four days after MCAo, $BrdU^+$ cells were seen in the ischemic core (Fig. 6C, D-E) and at the margins of the infarction, which was surrounded by astrocytes (Fig. 6E). By cell counting, we estimated that 7.0±1.6% (mean±SD, n=6 mice) of the cell nuclei in the ischemic tissue incorporated BrdU at day 4 post-ischemia (Fig. 6I). In order to find out whether the infiltrated monocytes proliferated, ischemic mice that had received adoptive transfer of DsRed monocytes at day one post-ischemia were injected BrdU at day two or four post-ischemia and were killed one hour later. Most DsRed cells did not show BrdU incorporation (Fig. 6F-H), with only 2% of $BrdU^+$ cells within the DsRed population four days post-ischemia (Fig. 6J). Assuming that the DsRed cells are a sample of the infiltrated monocytes, the percentage of proliferating monocytes should be similar to that of the DsRed population, indicating low monocyte proliferation at four days post-ischemia. However, BrdU incorporation was found in $DsRed^-$ $Iba1^+$ cells, including cells showing very ramified morphology that were located at the edges of the infarcted core (Fig. 6K,L). The percentage of cells incorporating BrdU was significantly higher within the $Iba1^+$ population than within the DsRed population (Fig. 6J). Within the $BrdU^+$ cells, the percentage of cells

expressing Iba-1 at day 4 post-ischemia was 63±9%. A considerable amount of $BrdU^+$ cells (the remaining 37%) that were mainly located in the core of the lesion did not express Iba-1 at all (Fig. 6K, L), and we currently do not know the nature of these cells.

3.7 Infiltrated macrophages acquire the expression of markers of alternative polarization

Macrophages can become polarized to an alternatively activated M2 phenotype (Sica and Mantovani 2012). After brain ischemia, we detected the expression of markers of M2 polarization, such as arginase-1 (Arg-1) and the chitinase-like protein YM-1 (Loke et al., 2002; Mandrekar-Colucci et al., 2012), by examining their mRNA expression in the ischemic tissue (Fig. 7A). By immunofluorescence, $Arg1^+$ cells showing different levels of expression of Iba-1 were detected within the ischemic tissue 4 days post-ischemia (Fig. 7B), and they were often seen surrounding blood vessels (Fig. 7C). By ICS-flow cytometry, Arg-1^+ cells ($CD11b^{hi}CD45^{hi}Ly6G^-$) were found in the ipsilateral brain hemisphere, but not in the contralateral hemisphere or the blood. After adoptive transfer of CD45.1 monocytes, $Arg1^+CD45.1^+$ infiltrated reporter monocytes were found in the ischemic tissue but not in the blood (Fig. 7D, Supplementary Fig. 10), and a substantial proportion of these $Arg1^+$ CD45.1 cells were positive for F4/80 (Fig. 7E).

Following injection of reporter DsRed monocytes into recipient mice we saw Arg-1^+ DsRed cells in the ischemic tissue by confocal microscopy (Fig. 8 A-E). After cell counting (Fig. 8B), we estimated that the percentage of DsRed cells

that were Arg-1$^+$ increased from 13±8% one day after injection (Fig. 8A) to 43±7% 3 days later (mean±SEM, n=4 per time point) (Fig. 8C-E). Also, some DsRed cells were positive for the M2 marker YM-1 (Fig. 8F-H), and the proportion of DsRed$^+$ cells that were YM-1$^+$ increased from 1 to 3 days after administration (Fig. 8I). These results suggest that infiltrated monocytes progressively acquired the expression of markers of alternatively activated macrophages in the ischemic tissue. Arg-1 and YM-1 immunoreactivity was also detected in DsRed negative cells showing long and fine ramifications (Fig. 8J) located near the periphery of the infarcted region closer to the non-affected tissue. We cannot exclude that these latter cells originated from monocytes on the basis of the absence of DsRed expression, given that only a fraction of the infiltrated monocytes were DsRed$^+$. However, the fine ramified morphology of these cells was different from that exhibited by the DsRed$^+$ monocytes, suggesting that they might correspond to microglia. Therefore, these M2 markers seem to be expressed not only by the infiltrated monocytes but also by the resident reactive microglia surrounding the ischemic core.

4. DISCUSSION

In this study we characterized the response of the various subtypes of circulating monocytes (Geissmann et al., 2003) to brain ischemia after permanent MCAo in mice. The subset of immature pro-inflammatory Ly6C^{hi}CD43^{lo} monocytes predominantly infiltrating the ischemic tissue suffered progressive differentiation to macrophages and acquired the

expression of markers of an alternative phenotype, suggesting functions in tissue repair. The main recruitment of Ly6C^{hi} monocytes and negligible infiltration of Ly6C^{lo} monocytes agrees with previous reports in experimental models of brain ischemia (Gliem et al., 2012; Kim et al., 2014; Michaud et al., 2014) and hemorrhage (Hammond et al., 2014). Circulating Ly6C^{hi}CD43^{lo} monocytes have a pro-inflammatory profile but subsequently maturate towards Ly6C^{lo}CD43^{hi} monocytes showing that high Ly6C expression marks an immature stage of blood monocytes, in agreement with previous observations in other experimental settings (Sunderkötter et al., 2004; Lee et al., 2009). Ly6C^{hi} cells express CCR2 and are prone to infiltrate to the inflamed tissues that release CCL2 or CCL7 chemokines (Tsou et al., 2007). Accordingly, the CCL2/CCR2 axis plays a crucial role in the migration of circulating leukocytes to the brain after ischemia (Dimitrijevic et al., 2007; Schilling et al., 2009; Schuette-Nuetgen et al., 2011), hemorrhage (Hammond et al., 2014), and following traumatic brain injury (Hsieh et al., 2014; Morganti et al., 2015). A study published when we were preparing this manuscript reported that CCR2 inhibition worsened the brain injury one day after transient MCAo in mice (Chu et al., 2015). This latter finding disagrees with the view that CCR2^{+} monocytes play a detrimental pro-inflammatory role in the very acute phase following brain ischemia (Dimitrijevic et al., 2007), intracerebral hemorrhage (Hammond et al., 2014), and brain trauma (Hsieh et al., 2014; Morganti et al., 2015). Therefore, further studies are needed to find out the precise function of these monocytes in acute stroke.

In the sub-acute phase of stroke, infiltrated monocytes seem to exert beneficial effects by preventing hemorrhagic transformation after ischemia

(Gliem et al., 2012) and contributing to tissue repair after hemorrhage (Hammond et al., 2014). In our ischemia model, the Ly6C^{hi} pro-inflammatory monocytes recruited to the ischemic tissue progressively changed the typical blood phenotype by down-regulating the expression of Ly6C and acquiring features of tissue macrophages. The loss of typical markers of circulating monocytes after brain infiltration was also reported after photothrombotic and transient ischemia (Gliem et al., 2012) and intracerebral hemorrhage (Hammond et al., 2014). In addition, we found that a proportion of the infiltrated Ly6C^{hi} monocytes expressed Arg-1, while circulating Ly6C^{hi} monocytes did not. Furthermore, infiltrated monocytes also acquired the expression of YM-1. Arg-1 and YM-1 are typical markers of M2 types of alternative macrophage activation in mice (Loke et al., 2002). These M2-like macrophage phenotypes are involved in resolution of inflammation and tissue repair (Mantovani et al., 2013). The expression of markers of alternatively activated macrophages has been previously found in the ischemic brain tissue (e.g. Perego et al., 2011; Hu et al., 2012; Zarruk et al., 2012; Pérez-de-Puig et al., 2013). A peak of M2-like cells was reported between 2 days (Perego et al., 2011) and 5 days (Hu et al., 2012) post-ischemia and it was followed by a down-regulation suggestive of a transient anti-inflammatory response with a specific time-window. In contrast to this M2 response, one study reported a persistent expression of certain M1 genes until at least 14 days in a model of transient MCAo in mice (Hu et al., 2012).

Regarding the contribution of macrophages versus microglia to the M2 phenotype, recent studies reported that repressing monocyte infiltration by pharmacological inhibition of CCR2 after traumatic brain injury (Morganti et

al., 2015) or transient MCAo (Chu et al., 2015) in mice reduced the brain expression of genes associated with M2 polarization, thereby supporting the involvement of infiltrating macrophages in this process. Overall, our results demonstrate that pro-inflammatory Ly6C^{hi}CD43^{lo} monocytes progressively differentiate to macrophages expressing markers of alternative activation. Nevertheless, expression of these M2 markers was also found in ramified cells located at the borders of the infarction suggesting that both macrophages and microglia can acquire the expression of M2 markers several days after stroke. It is becoming increasingly apparent that there are multiple macrophage phenotypes in the ischemic brain tissue based on the expression of several markers (Matsumoto et al., 2015). These observations agree with the concept that the M1/M2 classification is actually insufficient to designate the ensemble of phenotypes that microglia and macrophages can acquire under disease conditions.

Infiltrated leukocytes seem to predominate over resident microglia in the core of infarction after permanent ischemia as assessed using EYFP transgenic bone marrow chimeras (Tanaka et al., 2003), but the subtypes of infiltrated monocytes were not identified. By i.v. administration of reporter Ly6C^{hi} monocytes we show their presence in the ischemic core. In contrast to permanent ischemia, in ischemia/reperfusion models activated microglia showing morphological changes (e.g. retraction of cellular processes), phagocytic activity, and proliferation is described as predominant in the core of the lesion over that of infiltrated macrophages (Schilling et al., 2005; Denes et al., 2007). This difference between transient and permanent ischemia models might be attributable to a lower adaptive capacity of microglia

compared to macrophages to resist severe ischemic conditions (Matsumoto et al., 2007, 2008). Under these circumstances reactive microglia would preferentially accumulate at the periphery of infarction. After BrdU administration, we detected active proliferation in Iba-1 negative cells located in the infarcted core, and in ramified cells strongly positive for Iba-1 located at the periphery of the infarction. However, the reporter monocytes showed little BrdU incorporation. The finding that the proportion of cells showing BrdU incorporation was lower within the population of reporter monocytes than within the population of $Iba1^{+}$ cells suggests the possibility that reactive resident microglia could proliferate. This possibility agrees with the capacity of microglia for self-renewal that has been reported in other experimental situations (Ajami et al., 2007). Therefore, strong and persistent ischemic conditions seem to be favorable to blood-born macrophage differentiation in the core of the infarction while promoting microglia activation and, possibly, proliferation at the margins of infarction.

Blood monocytes cannot reach the vessels of the ischemic region through the local circulation since the ischemic core is devoid of blood flow. Extravasated monocytes were found at the leptomeninges and were seen on the basement membrane of the cortex and along the basal laminae of penetrating arterioles, progressively accessing deeper cortical locations. This finding agrees with previous observations in this experimental model showing neutrophil trafficking trough this pathway (Pérez-de-Puig et al., 2015). Infiltrating monocytes seemed to follow the tracks of the perforating vessels from the brain surface to deeper cortical zones, suggesting that regions surrounding the vasculature are permissive to cell migration. However, we cannot exclude

the possibility that circulating monocytes could also extravasate from perfused vessels in regions at the periphery of infarction and migrate to the ischemic core. Also, brain resident macrophages normally found in the perivascular spaces under physiological conditions could potentially reach the ischemic brain parenchyma, but in this study we could not specifically follow the fate of these cells. The location of infiltrated monocytes surrounding the blood vessels suggests some interaction with the vasculature that could be related to the described protection of macrophages against hemorrhagic transformation following ischemic stroke (Gliem et al., 2012).

5. CONCLUSION

The circulating classic Ly6C^{hi}CD43^{lo}CCR2^{+} monocytes are immature cells that progressively maturate towards non-classic Ly6C^{lo}CD43^{hi}CCR2^{-} CD11c^{+}MHCII^{+} subsets in the blood. While the latter cells are unresponsive to the inflammatory stimuli, the former are attracted to the ischemic brain tissue, which releases chemokines such as CCL2. Monocytes are often located adjacent to the blood vessels. Migration of monocytes from the leptomeninges along the penetrating vessels provides a route of entrance of these cells to the ischemic tissue. Monocytes differentiate to macrophages and acquire the expression of M2 markers suggesting an alternative polarization favorable to tissue repair. We conclude that strategies aiming to down-modulate leukocyte infiltration need to adjust to their changing temporal course and assorted phenotype.

ACKNOWLEDGMENTS

Financed by the Spanish Ministries of Economy MINECO (SAF2011-30492, SAF2014-56279) and Health (FIS PI12/01437), and the European Community FP7 (InMiND project n°278850). We acknowledge the Image and Cytometry platforms of IDIBAPS, and the Confocal Microscopy Unit of the *Serveis Cientifico-Tècnics* of the University of Barcelona for technical help. F.M.M. was supported by the '*Red Invictus'* of the *Instituto de Salud Carlos III* (RD12/0014/0011). We thank A. Hernández and F. Ruiz for technical support, Dr. T. Santalucia for help in genotyping protocols, Dr. A. Celada for providing the DsRed mice, and Dr. V. Brait for useful comments. The authors declare no competing financial interests

REFERENCES

Ajami B, Bennett JL, Krieger C, Tetzlaff W, Rossi FM. Local self-renewal can sustain CNS microglia maintenance and function throughout adult life. Nat Neurosci. 2007;10:1538-1543.

Bamezai A, Goldmacher V, Reiser H, Rock KL. Internalization of phosphatidylinositol-anchored lymphocyte proteins. I. Documentation and potential significance for T cell stimulation. J Immunol. 1989; 143:3107-3116.

Bauer J, Huitinga I, Zhao W, Lassmann H, Hickey WF, Dijkstra CD. The role of macrophages, perivascular cells, and microglial cells in the pathogenesis of experimental autoimmune encephalomyelitis. Glia. 1995; 15: 437-446.

Campanella M, Sciorati C, Tarozzo G, Beltramo M. Flow cytometric analysis of inflammatory cells in ischemic rat brain. Stroke. 2002; 33:586-592.

Cardona AE, Huang D, Sasse ME, Ransohoff RM. Isolation of murine microglial cells for RNA analysis or flow cytometry. Nat Protoc. 2006; 1:1947-1951.

Cardona AE, Sasse ME, Liu L, Cardona SM, Mizutani M, Savarin C, Hu T, Ransohoff RM. Scavenging roles of chemokine receptors: chemokine receptor deficiency is associated with increased levels of ligand in circulation and tissues. Blood. 2008; 112:256-263.

Chu HX, Broughton BR, Ah Kim H, Lee S, Drummond GR, Sobey CG. Evidence That Ly6Chi Monocytes Are Protective in Acute Ischemic Stroke by Promoting M2 Macrophage Polarization. Stroke 2015; 46:1929-1937.

Chu HX, Kim HA, Lee S, Moore JP, Chan CT, Vinh A, Gelderblom M, Arumugam TV, Broughton BR, Drummond GR, Sobey CG. Immune cell infiltration in malignant middle cerebral artery infarction: comparison with transient cerebral ischemia. J Cereb Blood Flow Metab. 2014;34:450-459.

Denes A, Vidyasagar R, Feng J, Narvainen J, McColl BW, Kauppinen RA, Allan SM. Proliferating resident microglia after focal cerebral ischaemia in mice. J Cereb Blood Flow Metab. 2007; 27:1941-1953.

Dimitrijevic OB, Stamatovic SM, Keep RF, Andjelkovic AV. Absence of the chemokine receptor CCR2 protects against cerebral ischemia/reperfusion injury in mice. Stroke, 2007; 38:1345-1353.

Geissmann F, Jung S, Littman DR. Blood monocytes consist of two principal subsets with distinct migratory properties. Immunity. 2003; 19:71-82.

Gelderblom M, Leypoldt F, Steinbach K, Behrens D, Choe CU, Siler DA, Arumugam TV, Orthey E, Gerloff C, Tolosa E, Magnus T. Temporal and spatial dynamics of cerebral immune cell accumulation in stroke. Stroke. 2009; 40:1849-1857.

Gliem M, Mausberg AK, Lee JI, Simiantonakis I, van Rooijen N, Hartung HP, Jander S. Macrophages prevent hemorrhagic infarct transformation in murine stroke models. Ann Neurol. 2012; 71:743-752.

Hammond MD, Taylor RA, Mullen MT, Ai Y, Aguila HL, Mack M, Kasner SE, McCullough LD, Sansing LH. CCR2+ Ly6C(hi) inflammatory monocyte recruitment exacerbates acute disability following intracerebral hemorrhage. J Neurosci. 2014; 34:3901-3909.

Hsieh CL, Niemi EC, Wang SH, Lee CC, Bingham D, Zhang J, Cozen ML, Charo I, Huang EJ, Liu J, Nakamura MC. CCR2 deficiency impairs macrophage infiltration and improves cognitive function after traumatic brain injury. J Neurotrauma. 2014; 31:1677-1688.

Hu X, Li P, Guo Y, Wang H, Leak RK, Chen S, Gao Y, Chen J. Microglia/macrophage polarization dynamics reveal novel mechanism of injury expansion after focal cerebral ischemia. Stroke. 2012; 43:3063-3070.

Kim E, Yang J, Beltran CD, Cho S. Role of spleen-derived monocytes/macrophages in acute ischemic brain injury. J Cereb Blood Flow Metab. 2014; 34:1411-1419.

Lee PY, Li Y, Kumagai Y, Xu Y, Weinstein JS, Kellner ES, Nacionales DC, Butfiloski EJ, van Rooijen N, Akira S, Sobel ES, Satoh M, Reeves WH. Type I interferon modulates monocyte recruitment and maturation in chronic inflammation. Am J Pathol. 2009; 175:2023-2033.

Loke P, Nair MG, Parkinson J, Guiliano D, Blaxter M, Allen JE. IL-4 dependent alternatively-activated macrophages have a distinctive in vivo gene expression phenotype. BMC Immunol. 2002; 3:7.

Mandrekar-Colucci S, Karlo JC, Landreth GE. Mechanisms underlying the rapid peroxisome proliferator-activated receptor-γ-mediated amyloid clearance and reversal of cognitive deficits in a murine model of Alzheimer's disease. J Neurosci. 2012; 32:10117-10128.

Mantovani A, Biswas SK, Galdiero MR, Sica A, Locati M. Macrophage plasticity and polarization in tissue repair and remodelling. J Pathol. 2013; 229:176-185.

Matsumoto H, Kumon Y, Watanabe H, Ohnishi T, Shudou M, Chuai M, Imai Y, Takahashi H, Tanaka J. Accumulation of macrophage-like cells expressing NG2 proteoglycan and Iba1 in ischemic core of rat brain after transient middle cerebral artery occlusion. J Cereb Blood Flow Metab. 2008; 28:149-163.

Matsumoto H, Kumon Y, Watanabe H, Ohnishi T, Shudou M, Ii C, Takahashi H, Imai Y, Tanaka J. Antibodies to CD11b, CD68, and lectin label neutrophils rather than microglia in traumatic and ischemic brain lesions. J Neurosci Res. 2007; 85:994-1009.

Matsumoto S, Tanaka J, Yano H, Takahashi H, Sugimoto K, Ohue S, Inoue A, Aono H, Kusakawa A, Watanabe H, Kumon Y, Ohnishi T. CD200+ and CD200- macrophages accumulated in ischemic lesions of rat brain: the two populations cannot be classified as either M1 or M2 macrophages. J Neuroimmunol. 2015; 282:7-20.

Merzaban JS, Burdick MM, Gadhoum SZ, Dagia NM, Chu JT, Fuhlbrigge RC, Sackstein R. Analysis of glycoprotein E-selectin ligands on human and mouse marrow cells enriched for hematopoietic stem/progenitor cells. Blood. 2011; 118:1774-1783.

Michaud JP, Pimentel-Coelho PM, Tremblay Y, Rivest S. The impact of Ly6Clow monocytes after cerebral hypoxia-ischemia in adult mice. J Cereb Blood Flow Metab. 2014; 34:e1-9.

Morganti JM, Jopson TD, Liu S, Riparip LK, Guandique CK, Gupta N, Ferguson AR, Rosi S. CCR2 antagonism alters brain macrophage polarization and ameliorates cognitive dysfunction induced by traumatic brain injury. J Neurosci. 2015; 35:748-760.

Ostberg JR, Barth RK, Frelinger JG. The Roman god Janus: a paradigm for the function of CD43. Immunol Today. 1998; 19:546-550.

Perego C, Fumagalli S, De Simoni MG. Temporal pattern of expression and colocalization of microglia/macrophage phenotype markers following brain ischemic injury in mice. J Neuroinflammation. 2011;8:174.

Pérez-de-Puig I, Miró-Mur F, Ferrer-Ferrer M, Gelpi E, Pedragosa J, Justicia C, Urra X, Chamorro A, Planas AM. Neutrophil recruitment to the brain in mouse and human ischemic stroke. Acta Neuropathol. 2015; 129:239-257.

Pérez-de-Puig I, Miró F, Salas-Perdomo A, Bonfill-Teixidor E, Ferrer-Ferrer M, Márquez-Kisinousky L, Planas AM. IL-10 deficiency exacerbates the brain inflammatory response to permanent ischemia without preventing resolution of the lesion. J Cereb Blood Flow Metab. 2013;33:1955-1966.

Polfliet MM, Goede PH, van Kesteren-Hendrikx EM, van Rooijen N, Dijkstra CD, van den Berg TK. A method for the selective depletion of perivascular and meningeal macrophages in the central nervous system. J Neuroimmunol. 2001; 116:188-195.

Schilling M, Besselmann M, Müller M, Strecker JK, Ringelstein EB, Kiefer R. Predominant phagocytic activity of resident microglia over hematogenous macrophages following transient focal cerebral ischemia: an investigation using green fluorescent protein transgenic bone marrow chimeric mice. Exp Neurol. 2005; 196:290-297.

Schilling M, Strecker JK, Ringelstein EB, Schäbitz WR, Kiefer R. The role of CC chemokine receptor 2 on microglia activation and blood-borne cell recruitment after transient focal cerebral ischemia in mice. Brain Res. 2009; 1289:79-84.

Schuette-Nuetgen K, Strecker JK, Minnerup J, Ringelstein EB, Schilling M. MCP-1/CCR-2-double-deficiency severely impairs the migration of hematogenous inflammatory cells following transient cerebral ischemia in mice. Exp Neurol. 2012; 233:849-858.

Sica A, Mantovani A. Macrophage plasticity and polarization: in vivo veritas. J Clin Invest. 2012; 122:787-795.

Sunderkötter C, Nikolic T, Dillon MJ, Van Rooijen N, Stehling M, Drevets DA, Leenen PJ. Subpopulations of mouse blood monocytes differ in maturation stage and inflammatory response. J Immunol. 2004; 172:4410-4417.

Strauss-Ayali D, Conrad SM, Mosser DM. Monocyte subpopulations and their differentiation patterns during infection. J Leukoc Biol. 2007; 82:244-252.

Tanaka R, Komine-Kobayashi M, Mochizuki H, Yamada M, Furuya T, Migita M, Shimada T, Mizuno Y, Urabe T. Migration of enhanced green fluorescent protein expressing bone marrow-derived microglia/macrophage into the

mouse brain following permanent focal ischemia. Neuroscience, 2003; 117:531-539.

Tsou CL, Peters W, Si Y, Slaymaker D, Aslanian AM, Weisberg SP, Mack M, Charo IF. Critical roles for CCR2 and MCP-3 in monocyte mobilization from bone marrow and recruitment to inflammatory sites. J Clin Invest. 2007; 117:902-909.

Urra X, Villamor N, Amaro S, Gómez-Choco M, Obach V, Oleaga L, Planas AM, Chamorro A. Monocyte subtypes predict clinical course and prognosis in human stroke. J Cereb Blood Flow Metab. 2009; 29:994-1002.

Wang X, Yue TL, Barone FC, Feuerstein GZ. Monocyte chemoattractant protein-1 messenger RNA expression in rat ischemic cortex. Stroke, 1995; 26:661-665.

Woodman RC, Johnston B, Hickey MJ, Teoh D, Reinhardt P, Poon BY, Kubes P. The functional paradox of CD43 in leukocyte recruitment: a study using CD43-deficient mice. J Exp Med. 1998; 188:2181-2186.

Yang Y, Rosenberg GA. Blood-brain barrier breakdown in acute and chronic cerebrovascular disease. Stroke. 2011; 42:3323-3328.

Zarbock A, Ley K, McEver RP, Hidalgo A. Leukocyte ligands for endothelial selectins: specialized glycoconjugates that mediate rolling and signaling under flow. Blood. 2011; 118:6743-6751.

Zarruk JG, Fernández-López D, García-Yébenes I, García-Gutiérrez MS, Vivancos J, Nombela F, Torres M, Burguete MC, Manzanares J, Lizasoain I, Moro MA. Cannabinoid type 2 receptor activation downregulates stroke-

induced classic and alternative brain macrophage/microglial activation concomitant to neuroprotection. Stroke. 2012;43:211-9.

Ziegler-Heitbrock L, Ancuta P, Crowe S, Dalod M, Grau V, Hart DN, Leenen PJ, Liu YJ, MacPherson G, Randolph GJ, Scherberich J, Schmitz J, Shortman K, Sozzani S, Strobl H, Zembala M, Austyn JM, Lutz MB. Nomenclature of monocytes and dendritic cells in blood. Blood. 2010; 116:e74-80.

FIGURE LEGENDS

Figure 1. Ly6C^{hi}CD43^{lo} monocytes infiltrate the ischemic tissue. A) Features of the different monocyte subtypes. Classic CD11b^{hi}Ly6C^{hi}CD43^{lo} monocytes (upper row plots) express CCR2, but not CD11c or MHCII, while CD11b^{hi}Ly6C^{lo}CD43^{hi} (lower row plots) monocytes are CCR2^{-} and express CD11c and MHCII. B, C) Ischemia induces the expression of CCL2 mRNA (n=3 to 7 mice per time point) (B) and protein (n=4 mice per group) (C) in the ischemic or control tissue, at the indicated times. One-way ANOVA by time (B) or Mann-Whitney test (C) versus control ** $p<0.01$; *** $p<0.001$. D) Number of Infiltrated myeloid cells (CD11b^{hi}CD45^{hi}) in the ischemic (ipsilateral) and contralateral hemispheres in controls, and at days 1, 4 and 7 after ischemia (n=6 to 20 mice per time point). Two-way ANOVA by time and hemisphere. *$p<0.05$, **$p<0.01$ vs. non-ischemic control. E) Infiltrating monocytes were identified as CD11b^{hi}CD45^{hi}Ly6G^{-} and its subtypes were depicted by its expression on Ly6C and CD43. Bar graph represents the number of Ly6C^{hi}CD43^{lo} versus Ly6C^{lo}CD43^{hi} monocytes present in the ipsilateral and contralateral hemispheres at days 1, 4 and 7 after ischemia (n=6 to 20 mice per time point). Two-way ANOVA by time and monocyte subtype. *$p<0.05$, **$p<0.01$, ***$p<0.001$ versus Ly6C^{hi}CD43^{lo}. F-H) In brain tissue, microglia (CD11b^{dim}CD45^{lo}) cell number (F) in the ischemic (ipsilateral, ipsi) and contralateral (contra) hemispheres is not affected by clodronate liposomes. In contrast, the numbers of myeloid cells (CD11b^{hi}CD45^{hi}) (G) in the ipsilateral hemisphere tend to be reduced in the clodronate liposome group. (H) Clodronate liposomes significantly reduced

the numbers of infiltrated $Ly6C^{hi}CD43^{lo}$ monocytes. Two-way Anova by monocyte subtype and treatment, *p<0.05.

Figure 2. Tracking monocytes after adoptive transfer of CD45.1 reporter monocytes. A) $CD45.1^+$ monocytes from Ly5.1 congenic mice were isolated from the bone marrow ($Ly6C^{hi}$ >90%) and 1.5 x 10^6 cells were i.v. injected in wild type (Ly5.2) ischemic mice. B) Injected CD45.1 cells were distinguished from regular CD45.2 cells with a specific antibody, as illustrated for blood cells. C) CD45.1 monocytes were injected at day 3 after MCAo and were studied 1 or 4 days later, i.e. at days 4 and 7 after MCAo. D) The plots illustrate the brain cells of ischemic mice showing the presence of $CD11b^{hi}CD45.1^+$ cells in the group of mice receiving i.v. administration of CD45.1 monocytes. A group of ischemic mice that did not receive CD45.1 monocytes (indicated by 'No AT') was used as control. E) Quantification of the infiltrated monocytes show that most of the infiltrated CD45.1 cells were $Ly6C^{hi}CD43^{lo}$, while $CD45.1^+Ly6C^{lo}CD43^{hi}$ cells were hardly detected in the brain at days 1 (n=8 mice) and 4 (n=3 mice) after AT (two-way ANOVA by monocyte subset and time, subset effect ***p<0.001). F) Immunofluorescence showed isolated $CD45.1^+$ cells (green) in the ischemic brain (n=2 per time point) 1 (AT+1day) and 4 (AT+4days) days after the mice received adoptive transfer of CD45.1 monocytes the day after ischemia. 'No AT' indicates mice that did not receive adoptive transfer. Myeloid cells are stained with CD68 (red) and nuclei are stained with ToPro-3 (blue). Bar scale: 10 μm. G) One day after MCAo, mice received an MRI scan (T2w) to measure infarct volume. The mice were then randomly assigned to receive

an i.v. administration of saline or Ly6C^{hi}CD45.1 monocytes (n=5 per group). The mice were scanned again at days 3 and 7 post-ischemia. Monocyte administration did not change the progression of the brain lesion. H) After adoptive transfer of Ly6C^{hi}CD45.1^{+} monocytes at day 3 post-ischemia, we examined by flow cytometry the proportion of Ly6C^{hi} cells within the population of the infiltrated CD45.1 reporter monocytes one (n=6) and four (n=3) days after administration. The proportion of CD45.1 cells expressing Ly6C^{hi} decreased with time (Mann-Whitney test, * $p<0.05$).

Figure 3. Infiltrated Ly6C^{hi} monocytes acquire features of macrophages. A) Representative contour plots showing the presence of macrophages (CD11b^{+}F4/80^{+}) in the ipsilateral (ipsi) but not the contralateral (contra) hemisphere 4 days after MCAo. This population is largely depressed after i.v. administration of clodronate liposomes one day prior to ischemia. The proportion of macrophages shows a significant increase in the ipsilateral hemisphere (**$p<0.01$, n=8 mice) that is prevented by clodronate liposomes (n=3 mice) (one-way ANOVA $^{\&}p<0.05$). B) Representative contour plots of the monocytes (CD11b^{hi}CD45^{hi}Ly6G^{-}) expressing F4/80 in the ipsilateral brain hemisphere at days 1 and 7 post-ischemia. Quantification by percentage of F4/80+ cells amongst the monocyte population shows increases in the brain versus the blood. Furthermore, the mean fluorescence intensity (MFI) of F4/80^{+} monocytes is higher in the brain than in the blood. Two-way ANOVA by tissue and time, ** $p<0.01$, ***$p<0.001$, (n=7 mice per time point). C) F4/80 in brain infiltrated CD45.1 monocytes injected either the day of MCAo (3 h later) (AT day 0 MCAO) (n=7), or 6 days after MCAo (AT

day 6 MCAO)(n=4). The brain and the blood were analyzed 1 day later, i.e. 1 or 7 days post-ischemia. More $CD45.1^+$ cells express F4/80 in the brain than in the blood, and the intensity of expression of this marker increases in the brain cells from day 1 to day 7 post-ischemia. Analysis was by two-way ANOVA by tissue and time point (**$p<0.01$). D) Monocytes sorted from the bone marrow of reporter DsRed mice were injected into wild type mice either one day (n=4) (AT day 1) or three days (n=4) (AT day 3) post-ischemia, and all the brains were examined at day 4 post-ischemia. Red fluorescent cells (arrowheads) were found in the ischemic cortex by confocal microscopy. Bar scale: 10 μm.

Figure 4. Monocytes and the vasculature. The location of the DsRed monocytes was studied in the ischemic tissue in relation to the brain vasculature. Images are from mice receiving DsRed cell administration 1 day after ischemia. A-K) Staining with an antibody against α4-laminin (green) labeled the basement membrane of the cortex and the endothelial basal lamina of the blood vessels. Reporter DsRed monocytes (red, arrowheads) are seen around the cortical basal lamina (A-C) as well as adjacent to the vessel wall (D-I), and some of the red cells are seen separated from the vessels and appear free in the parenchyma (J, K). L) illustrates a DsRed monocyte in the track of a blood vessel where the basal lamina is discontinuous, two days post-ischemia. M-R) Staining with pan-laminin reveals the presence of DsRed cells in the internal (M) and external (N-Q) parts of the vascular basal lamina. Cell nuclei are stained with To-Pro3 (blue). R) The numbers of DsRed cells either attached to the vasculature or

free in the parenchyma was counted 2 (n=2) and, 4 (n=3) days after DsRed cell administration. The proportion of DsRed cells adjacent to the vessels decreased with time. (* $p<0.05$, Two-way Anova by location and time point). Bar scale: 10 μm.

Figure 5. Infiltrated monocytes upregulate the expression of Iba-1. A-C) Iba-1 expression is strongly upregulated in the periphery of the infarction whereas the infarcted core contains cells expressing only low or moderate levels of Iba-1 four days after permanent MCAo. (B) Quantification of Iba-1$^+$ cells/area 4 days after MCAo shows a significantly higher density at the border of infarction than in the core (* $p<0.05$, Mann-Whitney test, n=4 mice). DsRed cells (arrowheads) are mainly located in the infarct core and in strongly positive Iba-1 border. DsRed cells show different levels of Iba-1 expression, ranging from 'no expression' (D, I) to 'low or intermediate expression' (E-H). Iba-1+ DsRed cells were more frequent three days after cell administration (F-I) than one day after administration (D-E). Images are representative of 8 mice. Cell nuclei are stained with To-Pro3 (blue). Bar scale: 50 μm in A and C; 10 μm in D-I.

Figure 6. Reporter monocytes do not show very active proliferation. BrdU (green) incorporation 2 (A-B) (n=3) and 4 (C-J) (n=6) days after MCAo. A,B) BrdU$^+$ cells surround the ischemic tissue 2 days after MCAo and are seen in the leptomeninges entering the brain following the penetrating cortical arterioles (arrows). C,D) Four days after MCAo, BrdU$^+$ cells reach

the ischemic core where they are seen in the brain parenchyma (arrowheads) (blood vessels are shown in red after vWF staining). E) $BrdU^+$ cells are rare in the zone of the astrocyte reaction (GFAP, red) located beyond the ischemic periphery 4 days following MCAo. F-H) After administration of DsRed monocytes one-day post-ischemia, BrdU incorporation (green, arrowheads) is seen in cells of the ipsilateral cortex, but the majority of DsRed cells (arrows) are not $BrdU^+$ at 4 (F,G) and 2 (H) days post-ischemia. One $BrdU^+DsRed^+$ cell is shown in (H) (arrowhead) to illustrate a low proportion of DsRed that were found to be $BrdU^+$. I) Quantification of the number of $BrdU^+$ cells out of total cell number per area shows a significant (*$p<0.05$, Mann-Whitney test, n=6) proportion of cells incorporating BrdU four days post-ischemia in the ischemic tissue but not in the contralateral hemisphere. J) The proportion of the DsRed reporter cells that was positive for BrdU was small, indicating that monocytes were not very proliferative 4 days post-ischemia. In contrast, a significantly higher (*<0.05, Mann-Whitney test, n=4 per group) percentage of $Iba1^+$ cells incorporated BrdU at this time. (K, L) BrdU immunoreaction (green) in sections of mice that did not receive DsRed monocyte administration (n=3). Ramified cells strongly immunoreactive for Iba-1 (red), with morphology compatible with reactive microglia (arrowheads), and mainly located at the periphery of infarction show BrdU incorporation 4 days after ischemia. The panels on the right are magnifications (x2) of the area in the square of the corresponding previous panel. Cell nuclei (To-Pro3) are shown in blue. Bar scale: 25 μm in A, C; 15 μm in E; 10 μm in B, D, F-H, K-L.

Figure 7. Ly6C^{hi} monocytes express Arginase-1 in the ischemic tissue but not in the blood. A) Time course mRNA expression of Arginase-1 (Arg-1), and YM-1, mRNA as quantified by qRT-PCR in control brain and the ipsilateral hemisphere at the indicated time points after MCAo (n=3-9 mice per time point). Values are expressed as fold versus control. One-way ANOVA followed by Dunnett's Multiple Comparison Test; **p<0.01, ***p<0.001. B) Representative confocal microscopy images from core and periphery of the ipsilateral and contralateral hemisphere 4 days after MCAo immunostained for Iba-1 (red) and Arg-1 (green). Cell nuclei are stained with Hoechst (blue) (n=8). Arg-1 is seen in cells expressing low levels of Iba-1 within the infarcted core. At the border of infarction cells are highly immunoreactive to Iba-1. Arg-1 immunoreactivity is not detected in the contralateral hemisphere. Bar scale: 15 μm. C) Immunofluorescence for Arg-1 (red) and pan-laminin (blue), which marks the basal laminae of blood vessels, shows Arg-1^{+} cells nearby the brain vasculature at days 1 (n=2 mice) and 4 (n=8 mice) post-ischemia. Bar scale: 10 μm. D,E) CD45.1 monocytes were injected i.v. to wild type mice either the day of MCAo (3 hours later, AT day 0 MCAO + 1d, n=5) or 6 days after MCAo (AT day 6 MCAO + 1d, n=4) and the brain and blood were analyzed by ICS-flow cytometry 1 day later. CD45.1 monocytes are not positive for Arg-1 in the blood, but a proportion of the CD45.1 monocytes express Arg-1 in the ischemic tissue (D), and most of these cells are F4/80^{+} (E). Differences in brain cell percentages between time points in (E) and (F) were not statistically significant, but a tendency for higher values at longer time points was observed.

Figure 8. M2 marker expression in infiltrated DsRed reporter monocytes. Monocytes isolated from the bone marrow of DsRed mice were injected i.v. to wild type mice one (n=4) (C-E, G-H, J) or 3 (n=4) (A, F) days after MCAo and the brain was studied by confocal microscopy at day 4 post-ischemia. Images show DsRed cells (red) and immunostaining for Arg-1 (green in A, C-E) or YM-1 (green in F-I). B) Cell number quantification shows that the proportion of DsRed cells that are Arg-1^+ significantly increases from one to three days after cell administration (Mann-Whitney test, *$p<0.05$). C-E) DsRed cells positive for Arg-1 (arrowheads). F-H) DsRed cells positive (arrowheads) for YM-1 (green). I) The proportion of DsRed cells positive for YM-1 shows significant increase from 1 to 3 days after cell administration (Mann-Whitney test, *$p<0.05$). J) shows a YM-1^+ cell (green) negative for DsRed (red) with a ramified morphology representative of cells located in the periphery of infarction. Cell nuclei are stained with To-Pro3 (blue). Bar scale: 10 μm.

Figure 1

Click here to download high resolution image

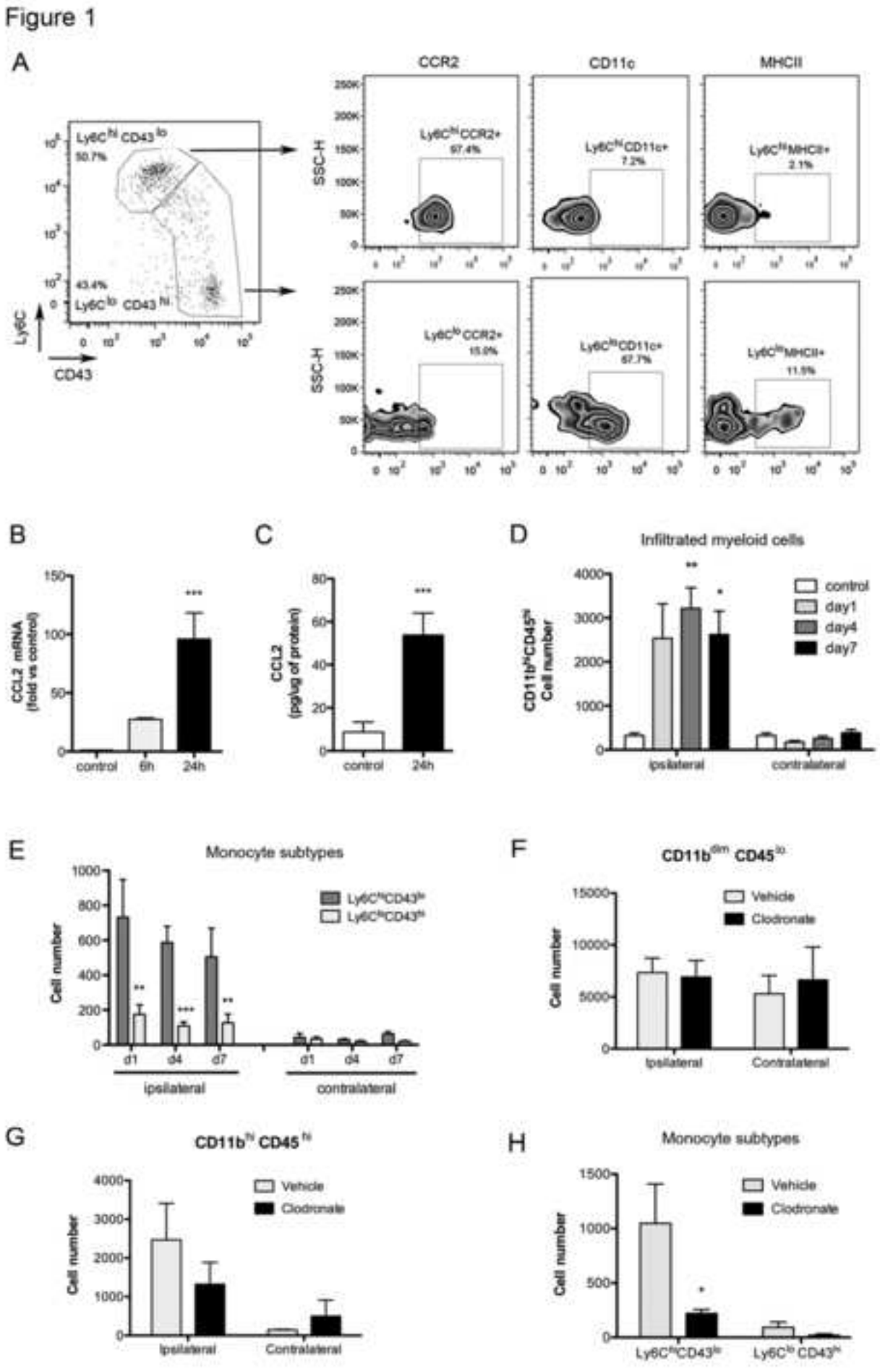

Figure 2

Click here to download high resolution image

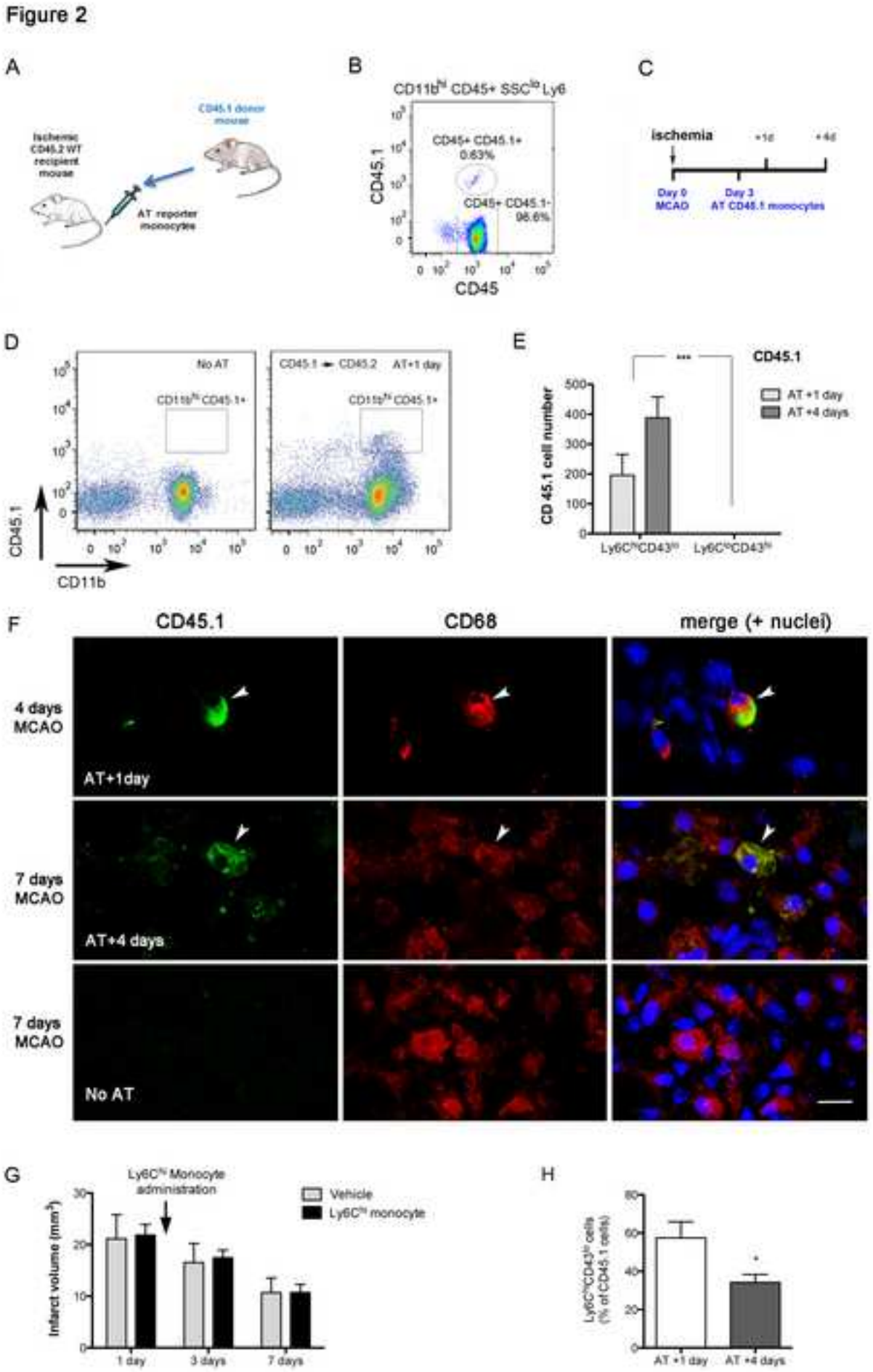

Figure 3

Click here to download high resolution image

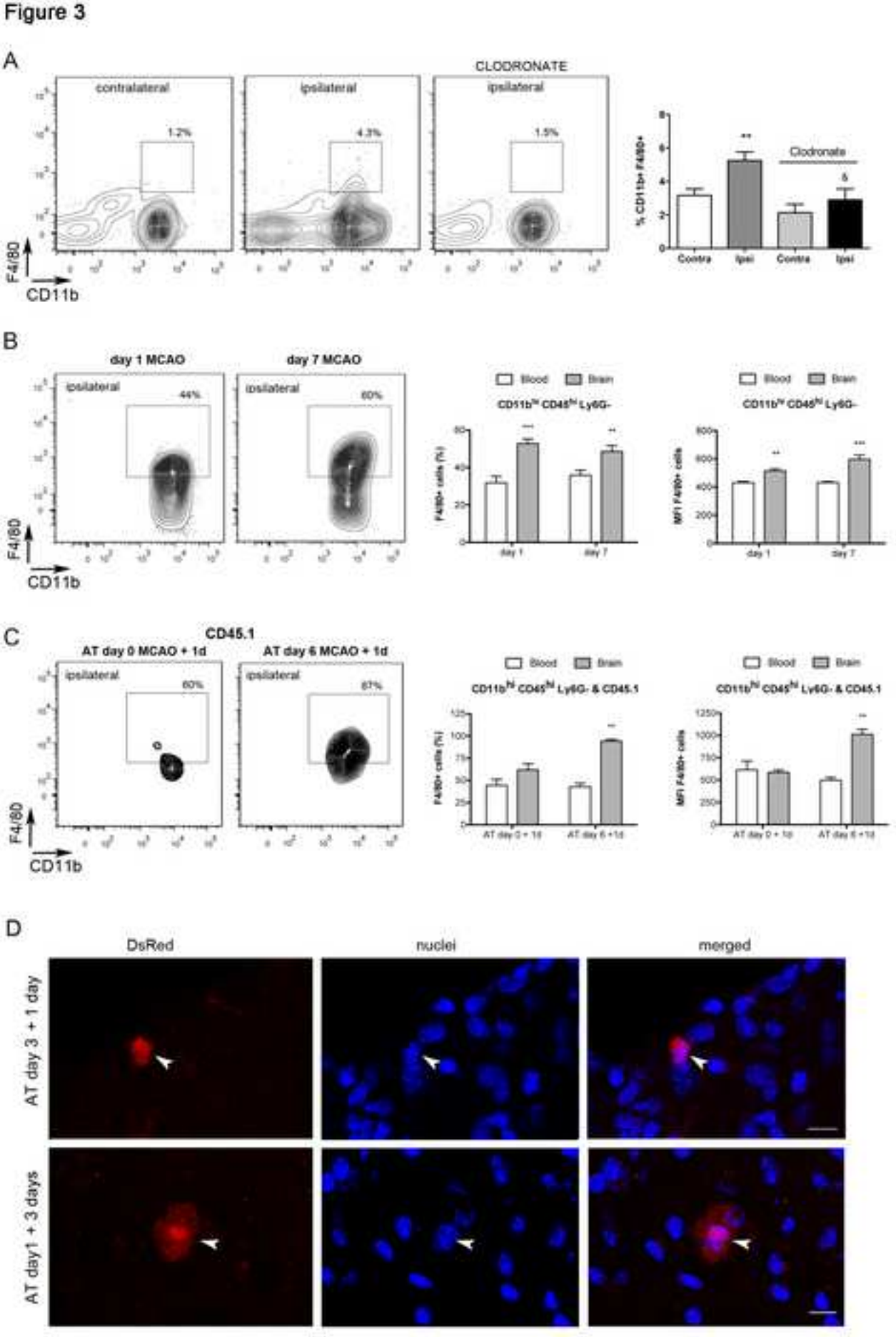

Figure 4

Click here to download high resolution image

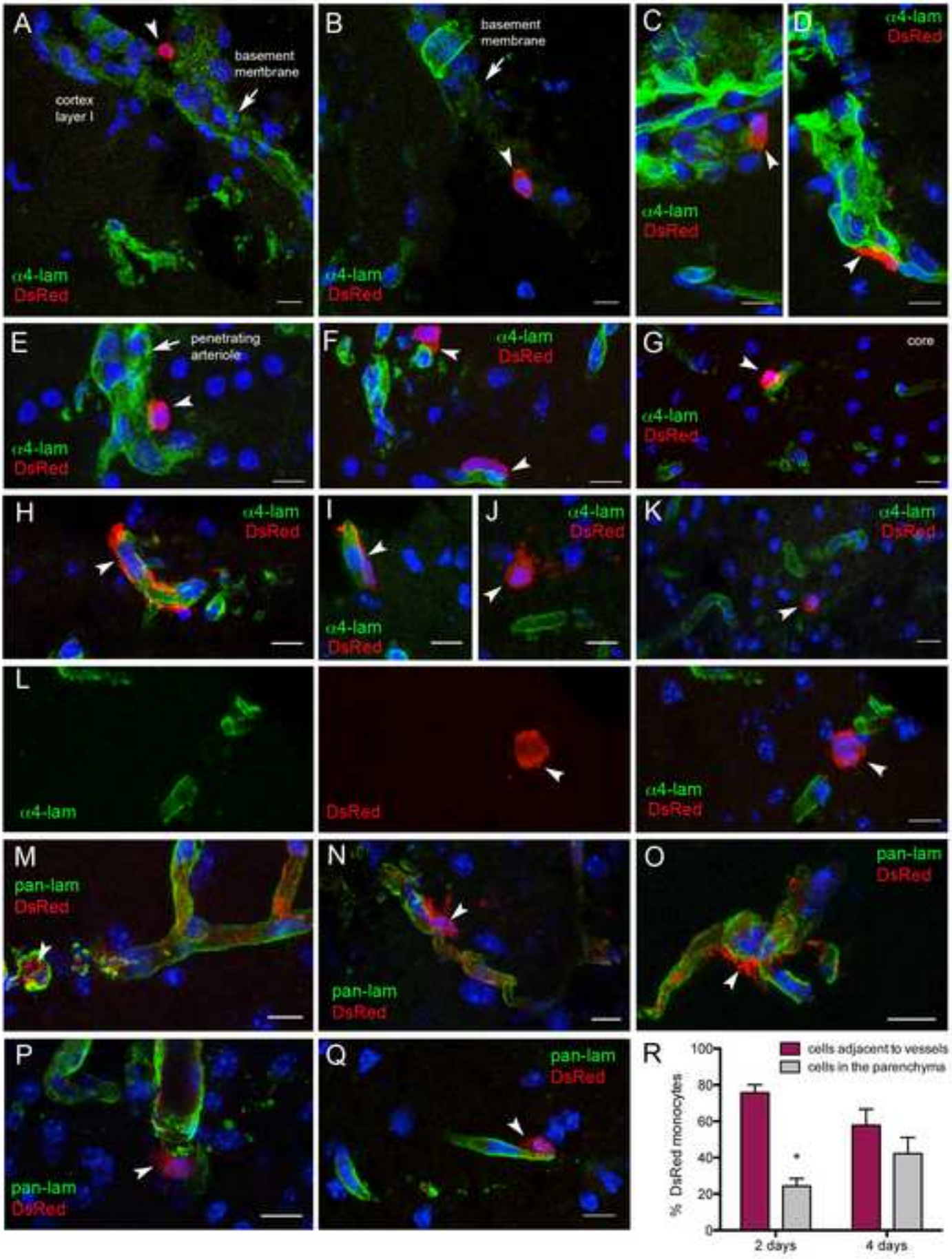

Figure 5

Click here to download high resolution image

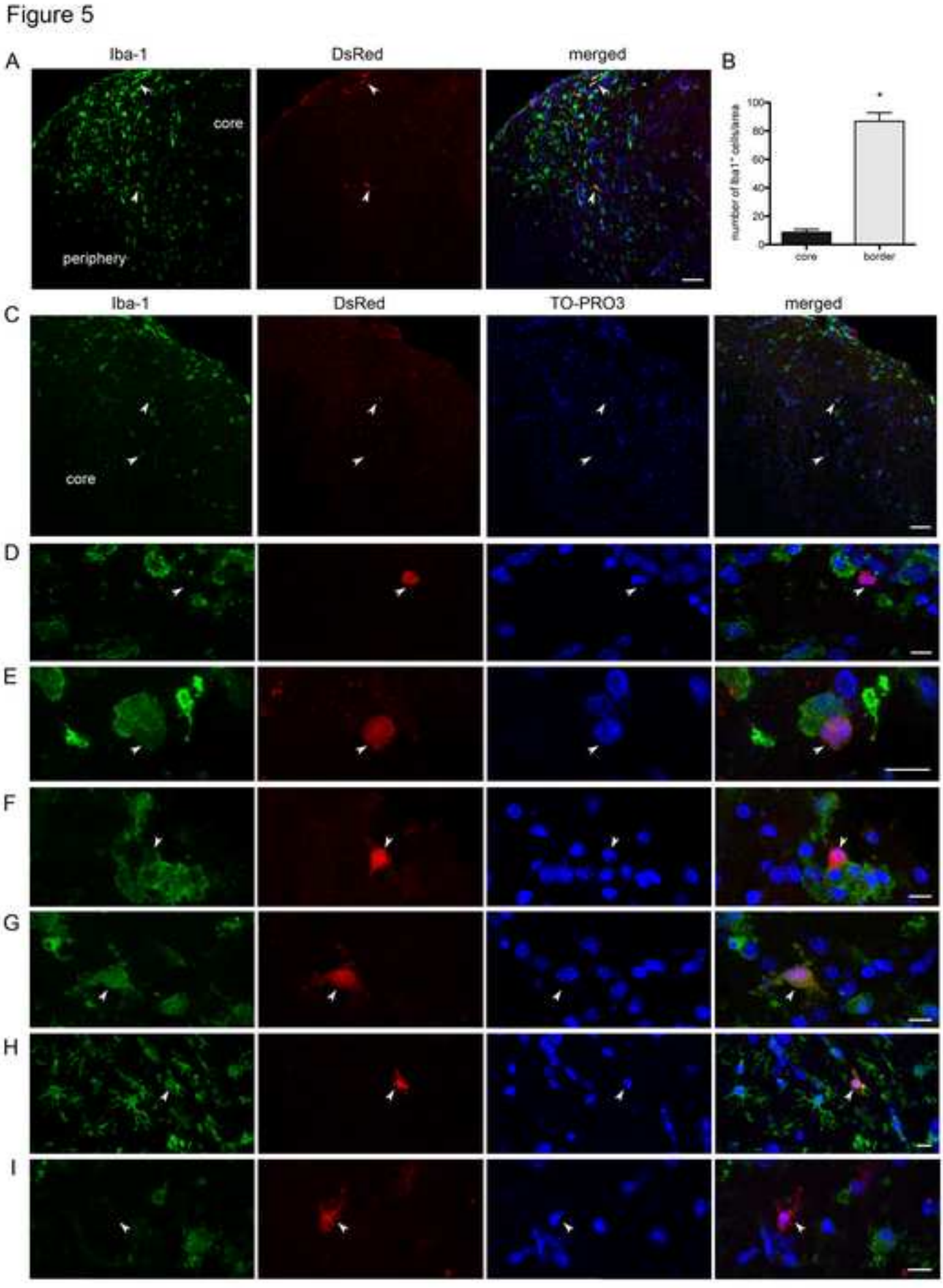

Figure 6

Click here to download high resolution image

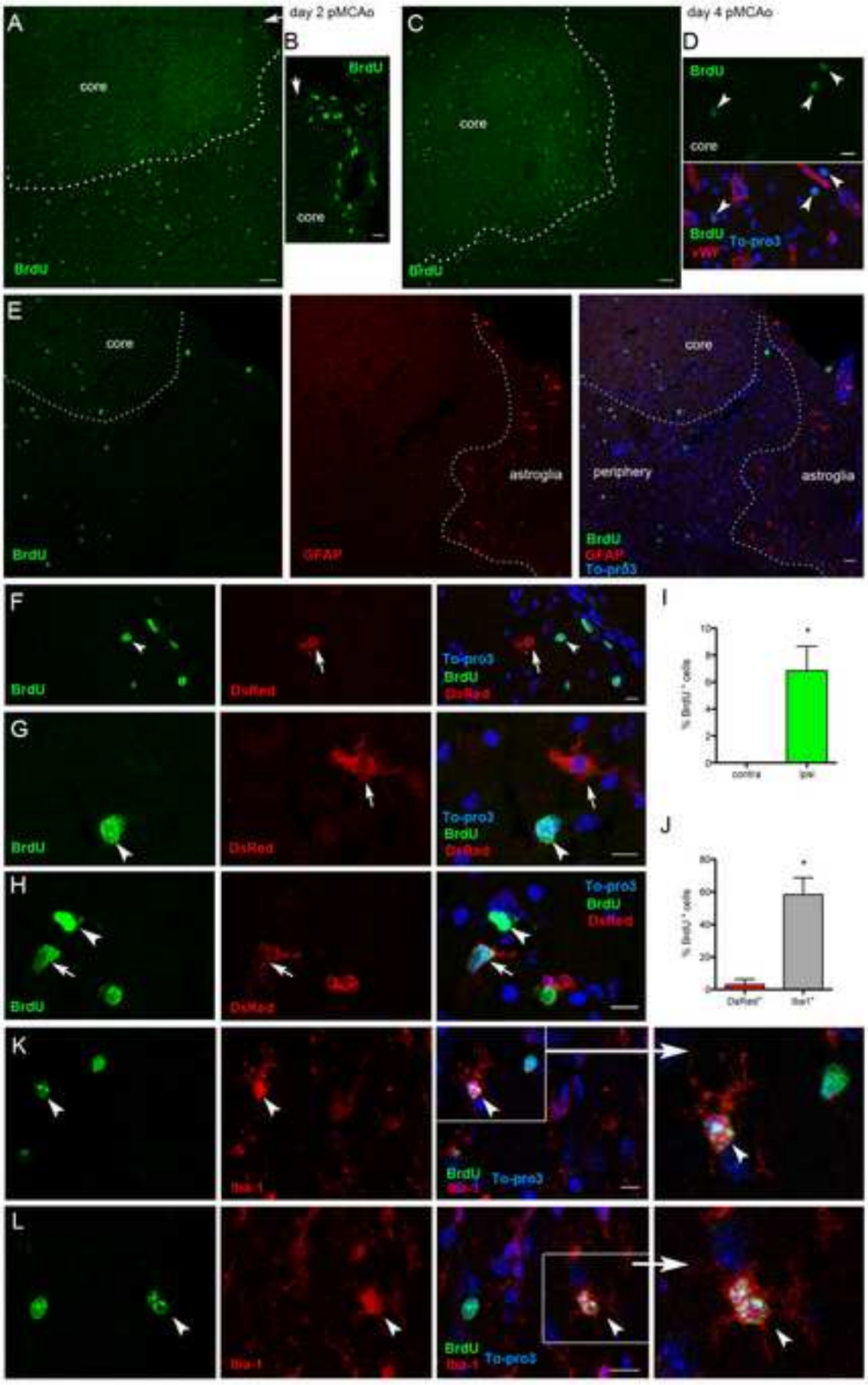

Figure 7

Click here to download high resolution image

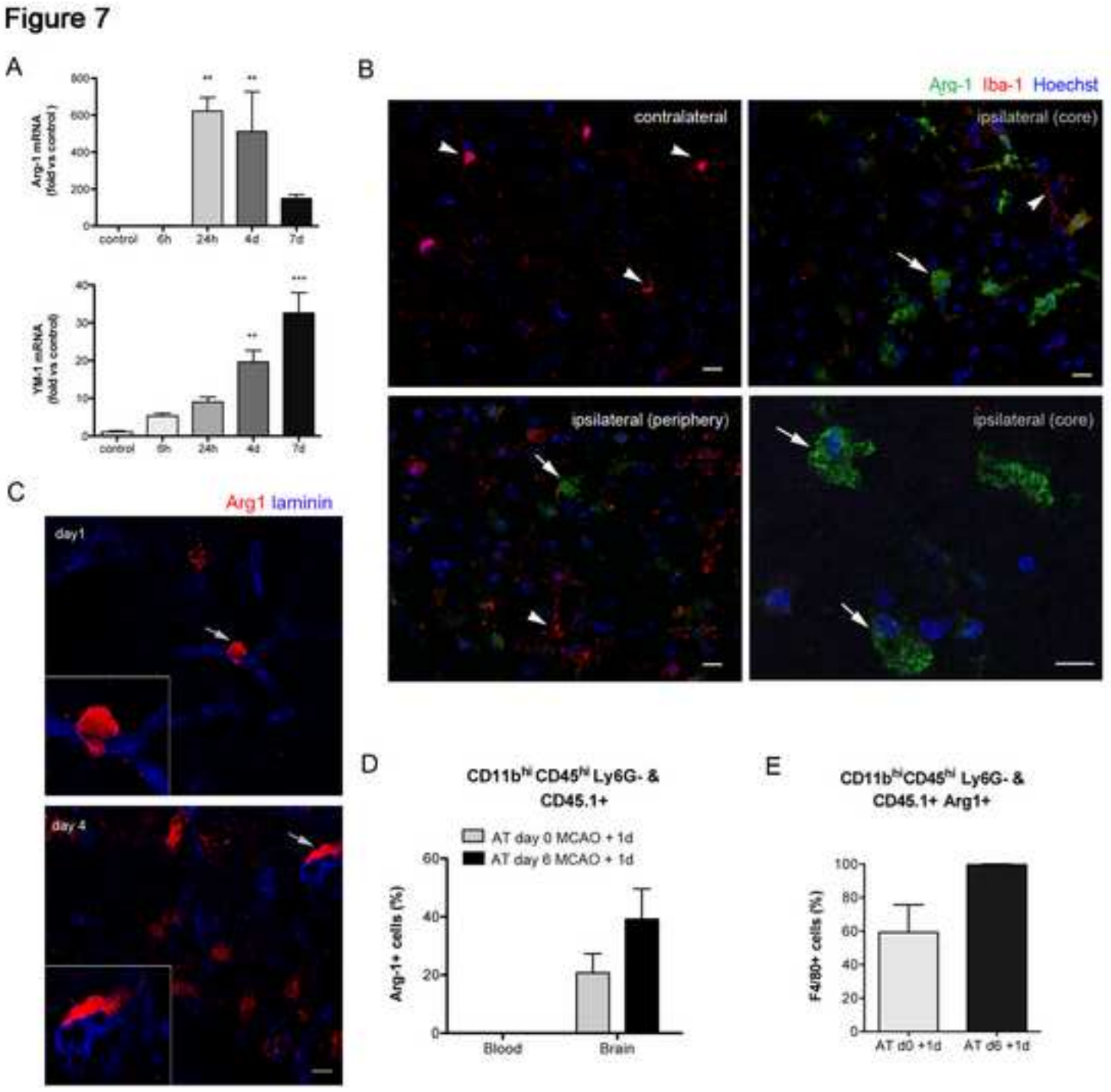

Figure 8

Click here to download high resolution image

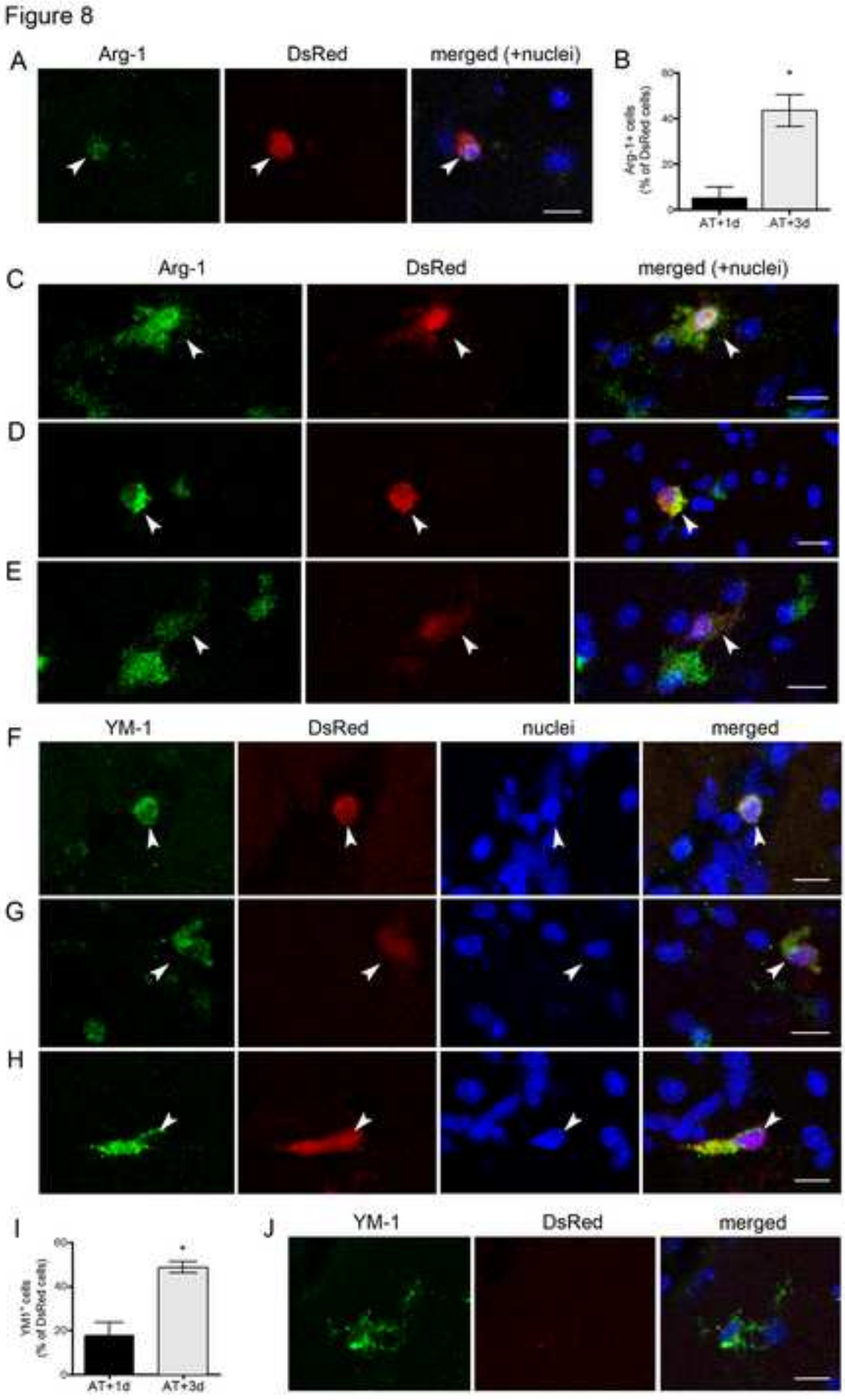

SUPPLEMENTARY FIGURES

Immature monocytes recruited to the ischemic mouse brain differentiate into macrophages with features of alternative activation

Francesc Miró-Mur[1,&], Isabel Pérez-de Puig[1,2,&], Maura Ferrer-Ferrer[1,2], Xabier Urra[1,3], Carles Justicia[1,2], Angel Chamorro[1,3], and Anna M. Planas[1,2*]

[1] Àrea de Neurociències, Institut d'Investigacions Biomèdiques August Pi i Sunyer (IDIBAPS), 08036-Barcelona, Spain
[2] Departament d'Isquèmia Cerebral i Neurodegeneració, Institut d'Investigacions Biomèdiques de Barcelona (IIBB), Consejo Superior de Investigaciones Científicas (CSIC), 08036-Barcelona, Spain
[3] Functional Stroke Unit of Cerebrovascular Diseases, Hospital Clínic, 08036-Barcelona, Spain

Supplementary Fig. 1

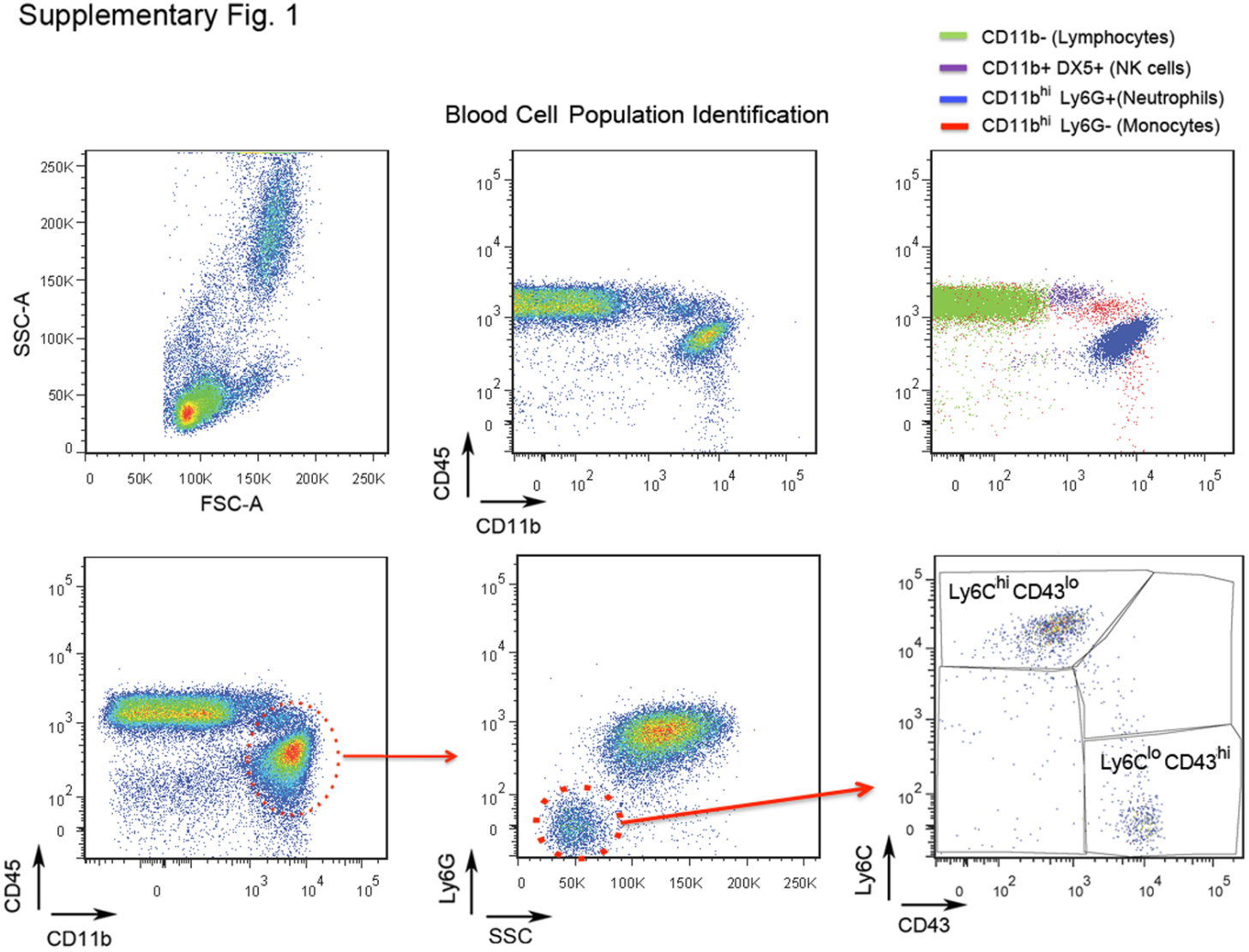

Supplementary Fig. 1: Gating strategy for the identification of cell populations in the blood.

Supplementary Fig. 2

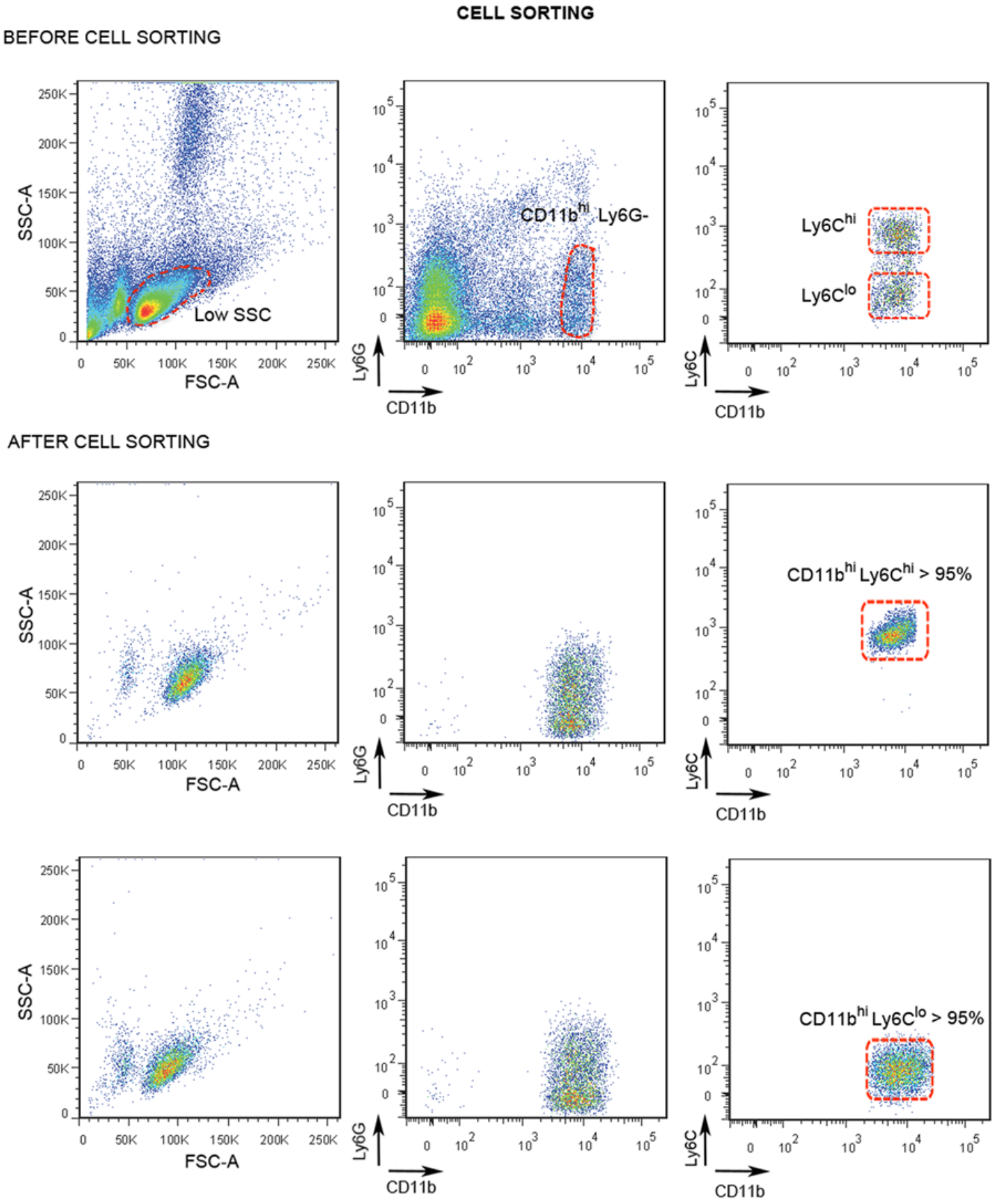

Supplementary Fig. 2: Cell sorting strategy to isolate monocyte subtypes from the blood according to their level of expression of Ly6C..

Supplementary Fig. 3

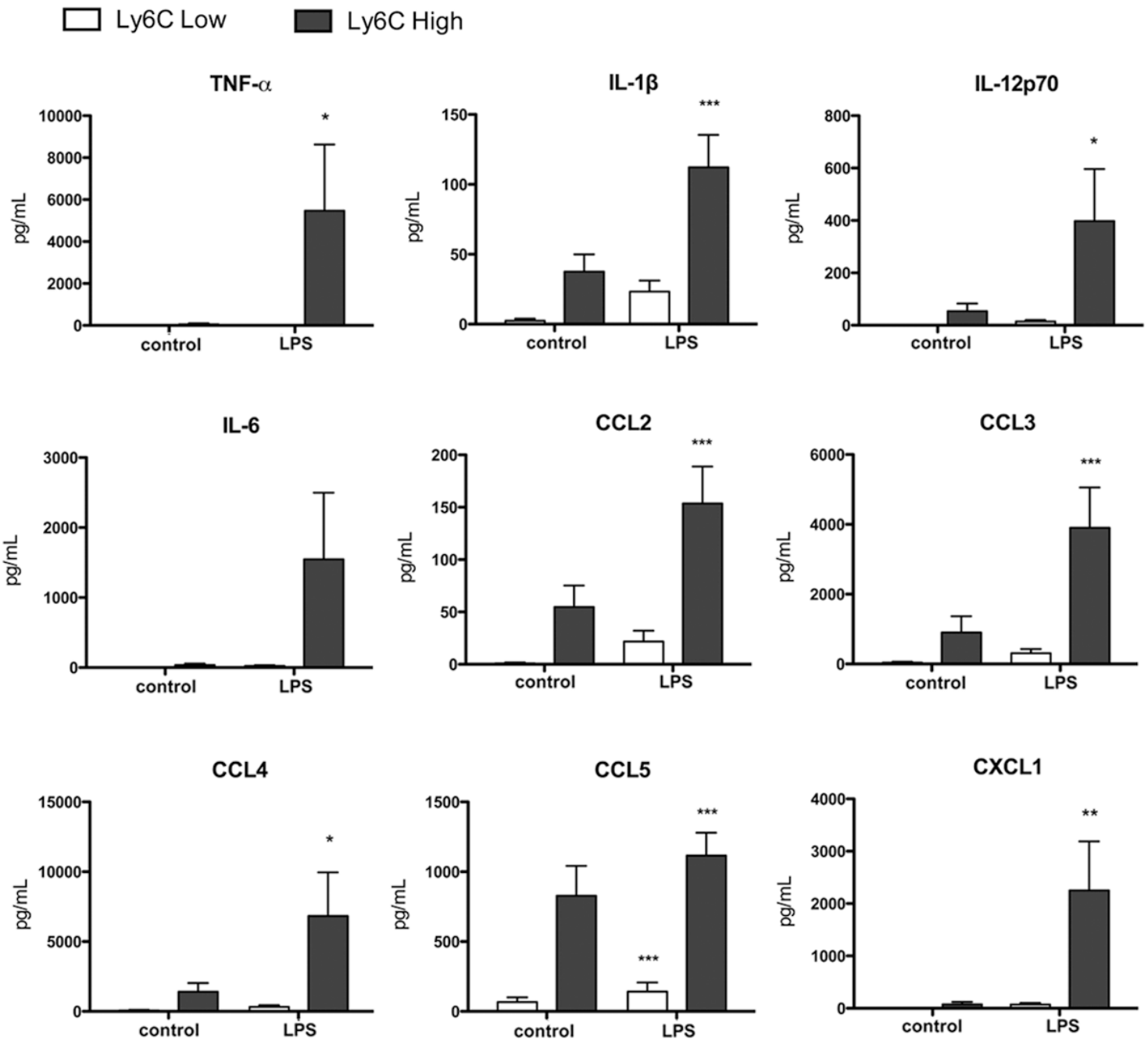

Supplementary Fig. 3: Cytokine release by monocyte subtypes. Ly6Chi and Ly6Clo monocytes were sorted from the blood or the spleen with positive selection. Each cell type was separately incubated in the presence or absence of LPS (100 ng/mL) for 18 hours and the cytokines and chemokines released to the culture medium were measured by Bio-plex ELISA assays (n=9 per treatment group and monocyte subset, obtained in 3 independent experiments). Ly6Chi monocytes showed a greater inflammatory response. *p<0.05; **p<0.01; ***p<0.001.

Supplementary Fig. 4

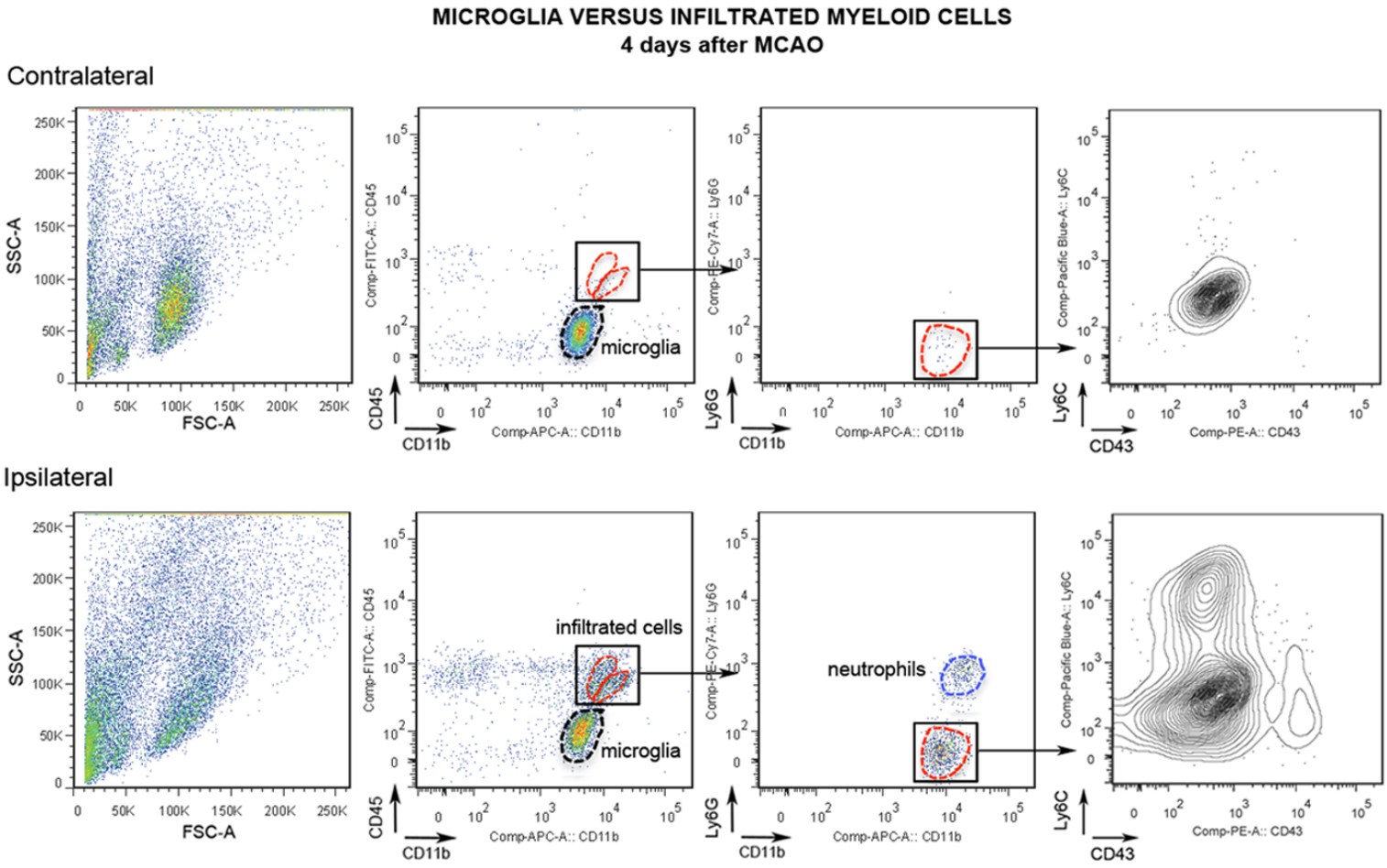

Supplemenrtary Fig. 4: Gating strategy to differentiate microglia from infiltrated myeloid cells in the brain tissue 4 days after MCAo.

Supplementary Fig. 5

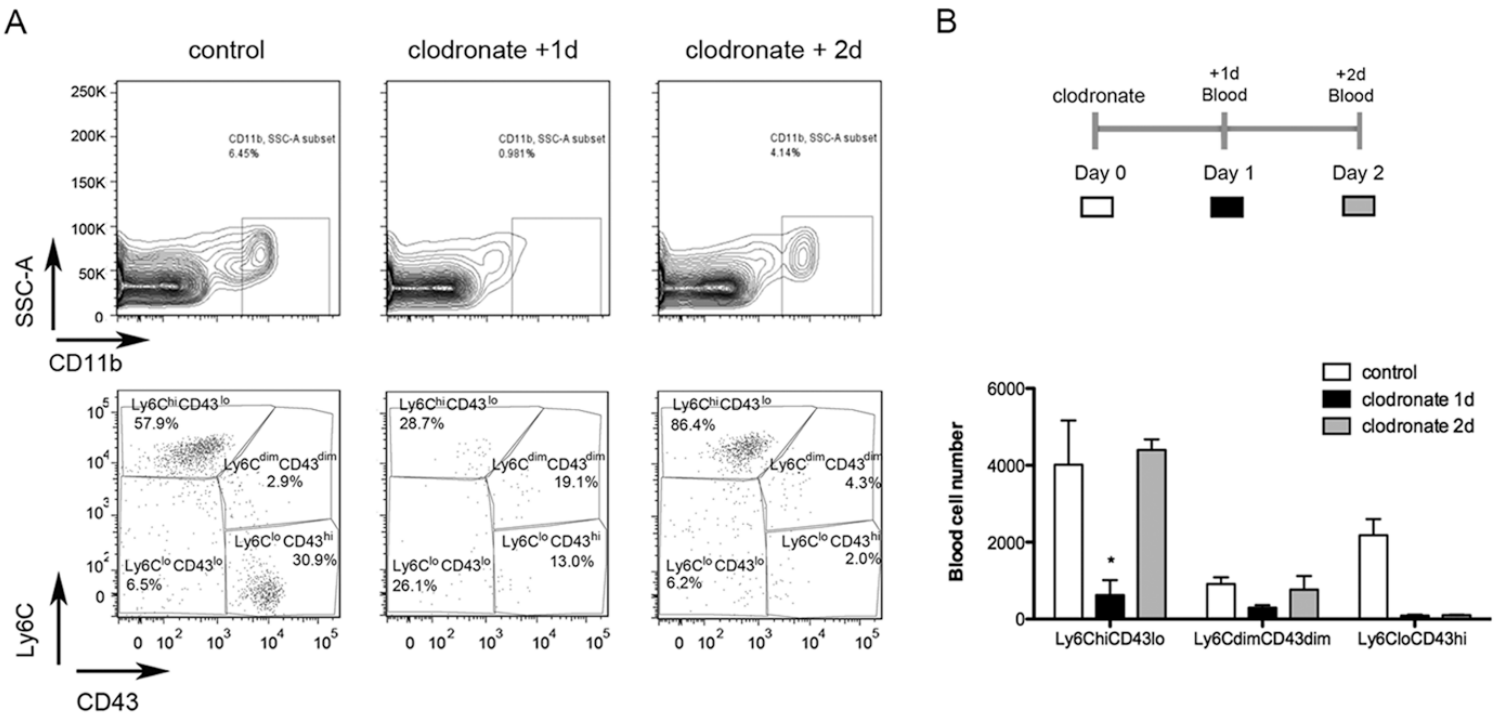

Supplementary Fig. 5: Effect of clodronate liposomes in blood. Mice received an i.v. administration of either clodronate liposomes or vehicle liposomes 1 day before MCAo (n=4-5 mice per group). (A) Blood monocyte subpopulations were assessed in control mice receiving i.v. clodronate liposome administration. Contour plots show clearance of blood monocytes 1 day after clodronate liposome administration (clodronate + 1d) but this cell population relapses after 2 days (clodronate + 2d). Representative dot plots illustrate that both Ly6Chi and Ly6Clo monocyte subpopulations are depleted one day after clodronate liposomes. However, at day 2, Ly6Chi cell numbers increase in the circulation likely due to new release from the body stores. (B) The bar graph summarizes the changes in monocyte subtype populations after injection of clodronate- or vehicle-liposomes (n=2 mice for every time-point and treatment, two-way ANOVA, *$p<0.05$).

Supplementary Fig. 6

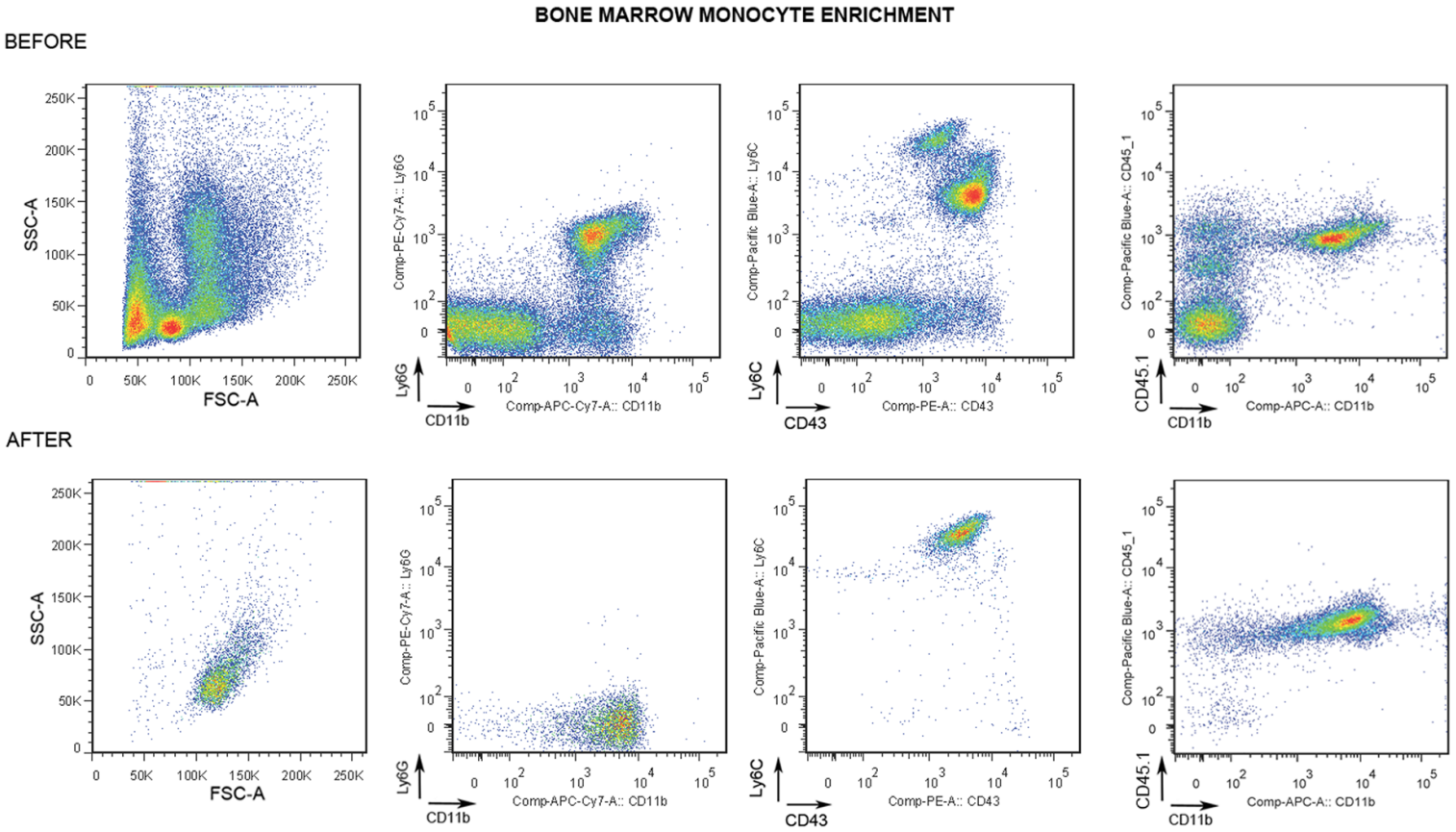

Supplementary Fig. 6: Monocytes were obtained from the bone marrow of Ly5.1 donor mice (before). The sorted CD45.1+ monocytes (after) were mainly Ly6Chi (90%).

Supplementary Fig. 7

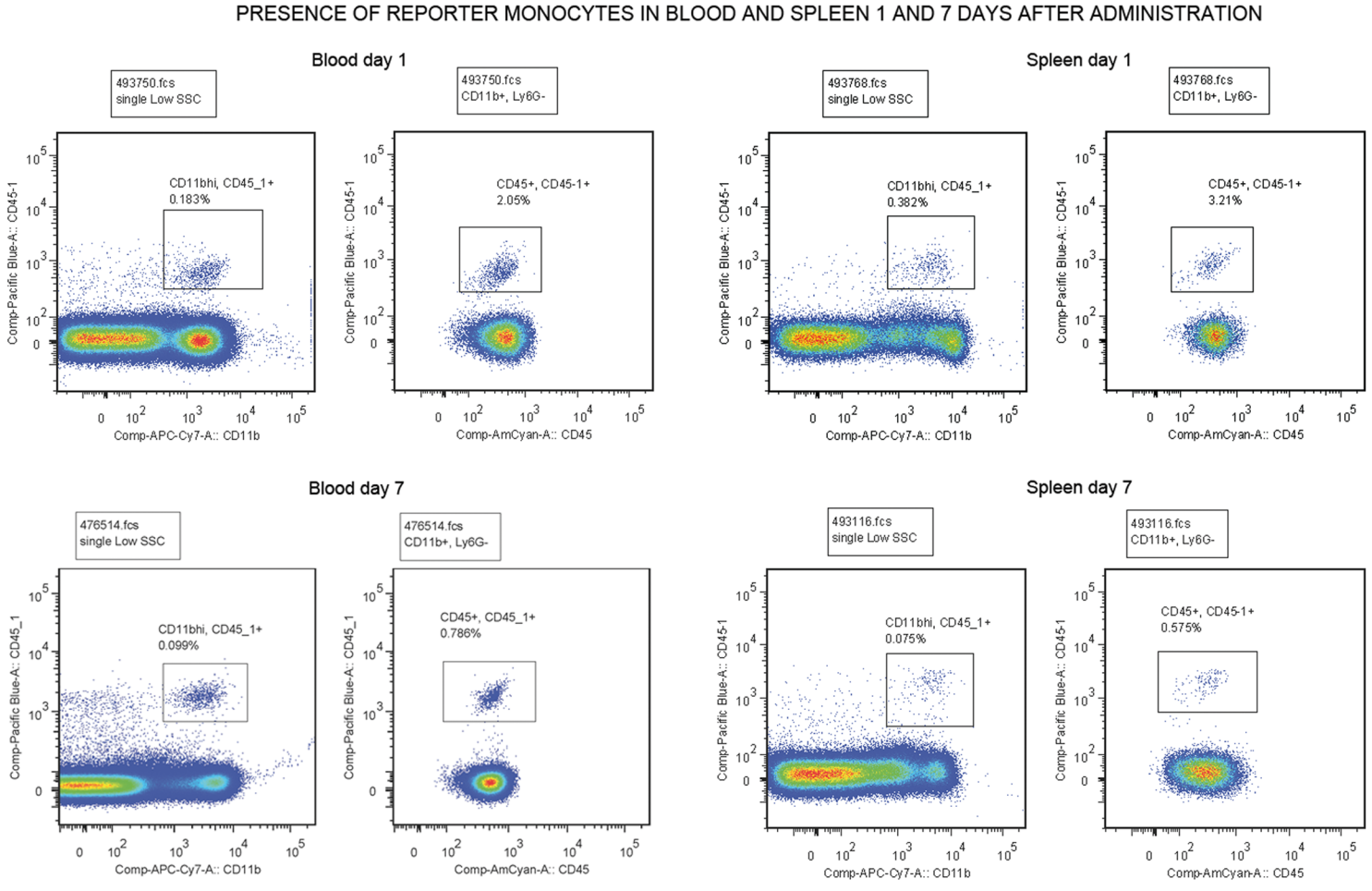

Supplementary Fig. 7 CD45.1 reporter monocytes in blood and spleen. Regular CD45.2 C57BL/6j mice (n=6) received an i.v. administration of CD45.1 reporter monocytes (1.5 x 10^6 cells) 3-4 hours after induction of ischemia. The presence of CD45.1+ cells in the blood and the spleen was studied 1 and 7 days later. Representative plots are shown illustrating that amongst the CD45+CD11b+ cells the percentage of CD45.1 reporter monocytes was 2-3% at day 1 and about 0.7% at day 7.

Supplementary Fig. 8

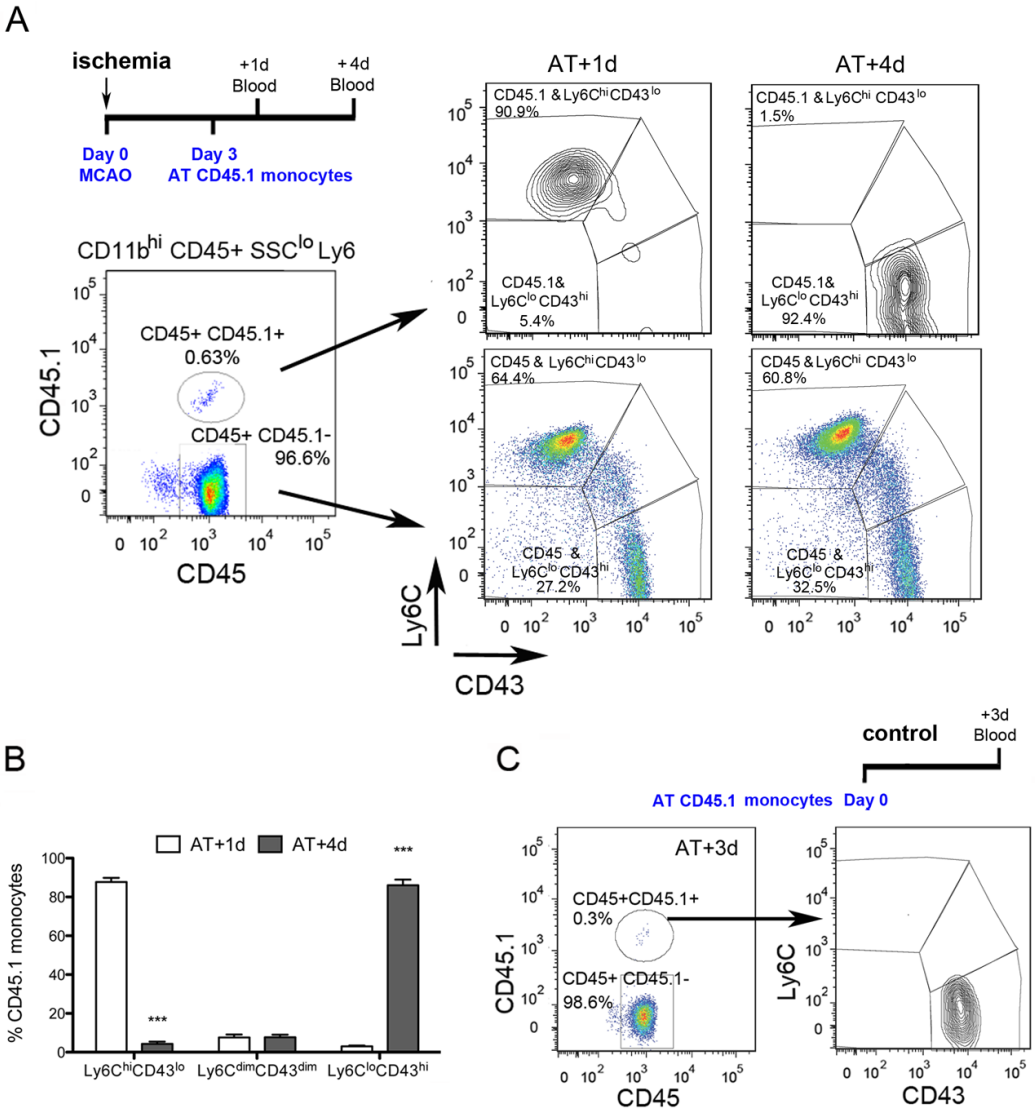

Supplementary Fig. 8: Tracking monocytes after adoptive transfer of CD45.1 reporter monocytes. A) CD45.1+ monocytes from Ly5.1 congenic mice were isolated from the bone marrow (Ly6Chi >90%) and 1.5 x 10^6 cells were i.v. injected in wild type (Ly5.2) mice at day 3 after MCAo. Adoptively transferred monocytes (AT) could be tracked by their expression of CD45.1. One day later (AT+1d), the CD45.1+ monocytes found in the blood were Ly6C^{hi} CD43^{lo} as the injected cells (n=4), but after 4 days more (n=6) (AT+4d), they became Ly6C^{lo} CD43^{hi} showing maturation from classical to non-classical subsets. B) Quantification shows significant differences in the proportion of the subtypes of CD45.1 monocyte between time points (Two-way ANOVA by time and monocyte subtype and Bonferroni post-hoc analysis, ***p<0.001). C) This phenomenon was also observed when CD45.1+ monocytes were adoptively transferred to control non-ischemic mice and the blood was analyzed after 3 days (AT+3d) (n=3).

Supplementary Fig. 9

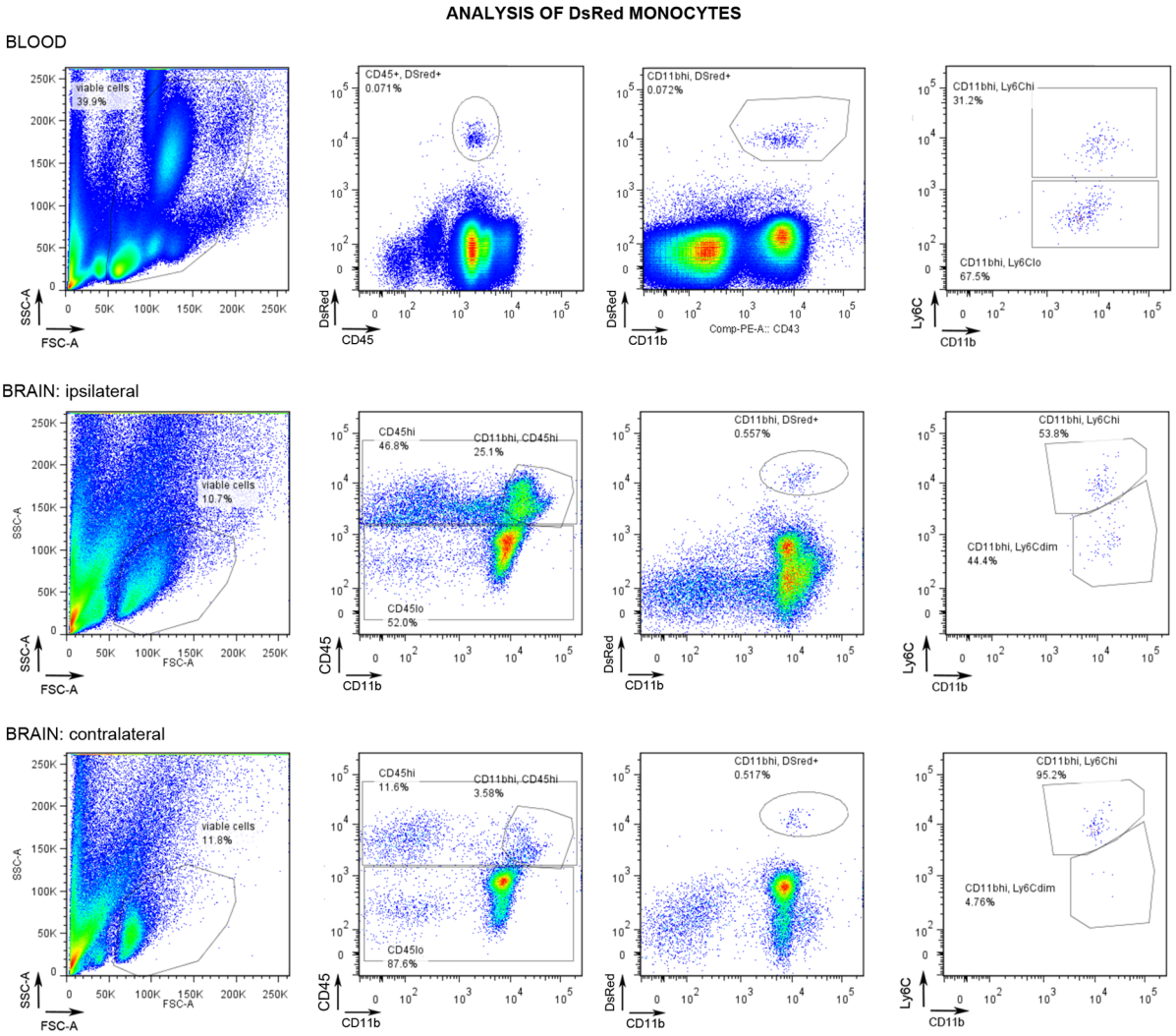

Supplementary Fig. 9: Wild type mice received injection of monocytes obtained from DsRed transgenic mice one day post-ischemia and the blood and brain were studied three days later. The gating strategy for the detection of DsRed monocytes is shown for blood and brain hemispheres. After 3 days, some of the injected Ly6Chi DsRed cells downregulated the expression of Ly6C, likely as part of their maturation process (see the text). Images are from one mouse representative of n=7 mice.

Supplementary Fig.10

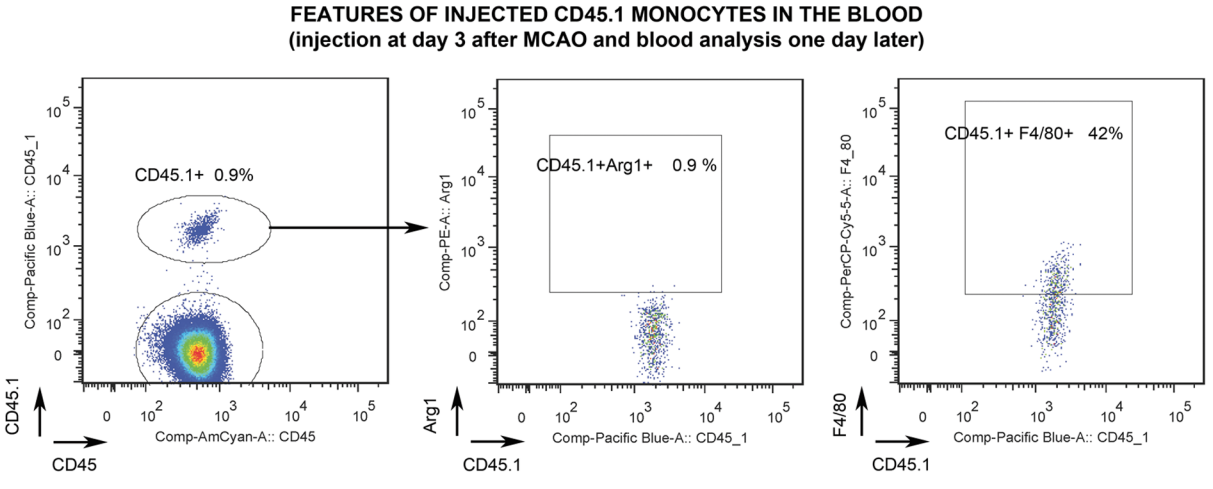

Supplementary Fig. 10: Wild type mice were administered i.v. with CD45.1 monocytes three days after MCAo and the blood was examined one day later by flow cytometry to examine the intracellular expression of Arg-1. The gating strategy is shown. In the blood, the CD45.1 monocytes did not express Arg-1, and a proportion of them expressed intermediate levels of F4/80.